

**Separation of caprolactam from water by membrane  
processes**

by

Min Guan

A thesis

presented to the University of Waterloo

in fulfillment of the

thesis requirement for the degree of

Master of Applied Science

in

Chemical Engineering

Waterloo, Ontario, Canada, 2013

© Min Guan 2013

## **Author's Declaration**

I hereby declare that I am the sole author of this thesis. This is a true copy of the thesis, including any required final revisions, as accepted by my examiners.

I understand that my thesis may be made electronically available to the public.

## Abstract

Caprolactam ( $C_6H_{11}NO$ , CPL) is the precursor to nylon 6. Production of caprolactam generates wastewater streams that contain a small amount of caprolactam. The objective of this study is to evaluate appropriate separation techniques to treat such wastewater and recover caprolactam from the wastewater for reuse.

Nanofiltration (NF) process was shown to be applicable to treat this caprolactam-containing wastewater, but the highest rejection of caprolactam reached only 70%. Operating conditions (e.g., transmembrane pressure, and caprolactam feed concentration) were shown to affect the performance of the NF process significantly. An increase in operating pressure improved the permeation rate, while both permeation rate and caprolactam rejection decreased with increasing feed caprolactam concentration. Surface fouling of the membrane also severely impeded NF operation. On the other hand, vacuum membrane distillation (VMD) offers a promising alternative that can filter out a high concentration of caprolactam from an aqueous solution. A higher operating temperature significantly increased the water permeation rate, while increasing feed caprolactam concentration lowered the permeation flux. Membrane fouling occurred during the concentration of caprolactam because the caprolactam solute deposited on the membrane surface, resulting in a decline in the VMD performance.

## **Acknowledgements**

I would like to express my sincerest appreciation and gratitude to my supervisor Professor Xianshe Feng for leading me to the world of membrane techniques. His invaluable guidance, constructive criticism and patient encouragement always supported me throughout my Master's studies. This thesis would not even exist without his unwavering guidance.

I would like to express my gratitude to the examination committee for their advices and comments on my thesis.

My deep appreciation also goes to all my friends in the membrane research group for their support and assistance.

To my family and friends, thanks for their endless trust and immeasurable love. This thesis is dedicated to them.

# Table of Contents

Author’s Declaration.....	ii
Abstract.....	iii
Acknowledgements.....	iv
Table of Contents .....	v
List of Figures.....	vii
List of Tables.....	ix
Chapter 1 Introduction .....	1
1.1 Background.....	1
1.2 Objectives of research .....	2
1.3 Outline of thesis .....	2
Chapter 2 Literature review .....	4
2.1 Overview of membrane separation technology.....	4
2.1.1 Pervaporation.....	7
2.1.2 Nanofiltration.....	9
2.1.3 Membrane distillation .....	10
2.2 Mass transport mechanism through membranes.....	12
2.2.1 Membrane transport in pervaporation .....	14
2.2.2 Membrane transport in nanofiltration.....	17
2.2.3 Membrane transport in membrane distillation.....	18
2.3 Polymers used as membrane materials.....	19
2.3.1 Polyamides .....	21
2.3.2 Polytetrafluoroethylene (PTFE) .....	24
2.4 Membrane contamination.....	27
2.4.1 Fouling and concentration polarization.....	27
2.4.2 Resistance-in-series model .....	31
2.4.3 Methods employed for fouling control.....	33
2.5 Removal of caprolactam from wastewater by membranes .....	34
Chapter 3 Experimental .....	36
3.1 Nanofiltration .....	36
3.1.1 Membranes .....	36

3.1.2 Nanofiltration experiments .....	37
3.2 Pervaporation .....	39
3.3 Vacuum membrane distillation.....	42
Chapter 4 Results and Discussion.....	44
4.1 Nanofiltration .....	44
4.1.1 Effect of operating conditions on nanofiltration performance .....	44
4.1.2 Fouling Resistance on nanofiltration membranes .....	55
4.2 Pervaporation .....	63
4.3 Vacuum membrane distillation.....	64
4.3.1 Effect of operating conditions on VMD performance .....	65
4.3.2 Concentration of aqueous solutions of caprolactam by VMD .....	71
Chapter 5 General conclusions and recommendations .....	75
5.1 General conclusions .....	75
5.2 Recommendations .....	76
References.....	78
Appendix A Sample Calculations .....	86
A.1 Resistance-in-series model calculations.....	86
A.2 Permeance calculations .....	87

## List of Figures

Figure 2.1 Schematic of a two-phase system separated by membrane (Mulder, 1991) .....	5
Figure 2.2 Categorizations of synthetic membranes (Pinnau and Freeman, 1999) .....	5
Figure 2.3 Schematic of membrane cross-sections (Mulder, 1991) .....	7
Figure 2.4 Schematic of pervaporation process .....	8
Figure 2.5 Schematic diagram of VMD (Alkhudhiri et al., 2012).....	11
Figure 2.6 Schematic of two types of membrane transport mechanism (Baker, 2004) ....	12
Figure 2.7 Schematic membrane transport models for different membrane processes (Wilderer, 2011) .....	14
Figure 2.8 Interfacial polymerization for membrane formation .....	23
Figure 2.9 Polyamide formation between PEI and TMC (Fang et al., 2013) .....	24
Figure 2.10 Major mass transfer resistances in porous membranes. $R_{cp}$ , $R_c$ , $R_m$ and $R_p$ represent resistance due to concentration polarization, cake layer formation, the membrane and pore-blocking, respectively. ....	29
Figure 2.11 Concentration profile build-up in boundary layer .....	30
Figure 2.12 Flux-applied pressure curves for pure water and a solution permeation.....	32
Figure 3.1 Schematic of nanofiltration setup .....	38
Figure 3.2 Schematic of pervaporation apparatus.....	41
Figure 4.1 Effect of operating pressure on permeation flux (a) and caprolactam rejection (b) at different feed caprolactam concentrations, Membrane 1 .....	45
Figure 4.2 Effect of operating pressure on permeation flux (a) and caprolactam rejection (b) at different feed caprolactam concentrations, Membrane 2 .....	46
Figure 4.3 Effect of operating pressure on permeation flux (a) and caprolactam rejection (b) at different feed caprolactam concentrations, Membrane NF1 .....	47
Figure 4.4 Effect of operating pressure on permeation flux (a) and caprolactam rejection (b) at different feed caprolactam concentrations, Membrane NF2 .....	48
Figure 4.5 Effect of operating pressure on permeation flux (a) and caprolactam rejection (b) at different feed caprolactam concentrations, Membrane NF-45.....	49
Figure 4.6 Schematic of reactant deposition sequence for membrane formation by interfacial polymerization .....	51
Figure 4.7 Pure water permeation results before and after caprolactam NF test in Membrane NF-45 .....	54
Figure 4.8 Membrane and fouling resistances as a function of pressure, Membrane 1 ....	56
Figure 4.9 Membrane and fouling resistances as a function of pressure, Membrane 2....	56
Figure 4.10 Membrane and fouling resistances as a function of pressure, Membrane NF1 .....	57
Figure 4.11 Membrane and fouling resistances as a function of pressure, Membrane NF2 .....	57

Figure 4.12 Membrane and fouling resistances as a function of pressure, Membrane NF-45 .....	58
Figure 4.13 $R_f/R_{total}$ ratio for various NF membranes as a function of operating pressure .....	59
Figure 4.14 Variation of fouling resistances as function of feed caprolactam concentration. Pressure 0.8MPa .....	60
Figure 4.15 Permeation flux (a) and permeation concentration (b) as a function of operating time, Membrane NF1, 1wt% feed caprolactam. Membrane was washed with distilled water between batch NF runs .....	62
Figure 4.16 Effects of temperature on water permeation flux in the PTFE membrane ....	67
Figure 4.17 Effects of temperature on water permeance in the PTFE membrane .....	67
Figure 4.18 Effects of feed concentration on water permeation flux in the PTFE membrane.....	70
Figure 4.19 Effects of feed concentration on water permeance in the PTFE membrane .	70
Figure 4.20 The permeation flux as a function of operating time, initial feed caprolactam concentration, 1 wt% .....	72
Figure 4.21 Concentration of caprolactam aqueous solution as a function of operating time, initial feed caprolactam concentration 1wt% .....	73
Figure 4.22 SEM image of the deposit formed on the membrane surface during the concentration of caprolactam solutions (Gryta, 2006).....	74



## List of Tables

Table 2.1 Typical properties of pressure-driven membranes (Shirazi et al., 2010) .....	9
Table 2.2 Physical properties of nylon 6 (Brandrup, 1999).....	21
Table 2.3 Physical properties of DuPont™ PTFE .....	25
Table 2.4 Surface tension of some liquids at 20°C (William et al., 2012) .....	26
Table 2.5 Surface energies of some polymers (Van Krevelen, 1972).....	27
Table 4.1 Comparison of caprolactam and water properties.....	65

# Chapter 1 Introduction

## 1.1 Background

As a precursor to nylon 6, caprolactam ( $C_6H_{11}NO$ , CPL) is extensively used in manufacturing nylon 6, which is used to make a broad variety of products ranging from fibers and yarns to engineering plastics. In the past decades, due to growth of population and progressive urbanization, there has been an increasing demand for caprolactam all over the world (Hong and Xu, 2012). In 2012, the production of caprolactam reached 5.68 million tons globally, and it is expected to continue to continuously in the future.

During caprolactam production, wastewater containing a low concentration of caprolactam is produced. The caprolactam present in the wastewater represents not only an economic loss but also a pollution hazard due to its toxic characteristics (Sheldon, 1989).

As a consequence, it is of interest to evaluate appropriate separation techniques to treat such wastewater while recovering caprolactam from the wastewater for reuse. Currently, bioremediation, solvent extraction and vacuum evaporation have been used to treat caprolactam-containing wastewater (Baxi and Shah, 2002; Chen et al., 2013). However, these methods are still not ideal for recovery of caprolactam from wastewater because of unfavorable process economics or use of additional chemicals.

Membrane processes have been evolved as a viable separation technique (Noble,

1987). They are physical processes, and often consume less energy with a better separation efficiency than conventional separation processes. Membranes can be considered as semi-permeable barriers that restrict certain molecules from passing through a membrane, thereby achieving separation. Membrane separation can occur based on the size exclusion, differences in diffusivity and solubility of the permeant in the membrane or both. Membrane processes can be divided into ultrafiltration (UF), microfiltration (MF), membrane distillation (MD), reverse osmosis (RO), nanofiltration (NF), electrodialysis (ED), gas separation (GS) and pervaporation (PV).

## **1.2 Objectives of research**

The purpose of this study is to investigate the performance of membrane processes for removal of small amounts of caprolactam from wastewater. Based on previous research (Denisova, 1999; Gryta, 2006; Zhang et al., 2007), caprolactam separation from water by nanofiltration (NF), pervaporation (PV) and vacuum membrane distillation (VMD) processes were specifically evaluated in this study. The effects of operating conditions (e.g., temperature and pressure) on the separation performance were studied for each membrane process. In addition, membrane fouling was also investigated to gain a better understanding of how fouling behavior influenced the separation performance.

## **1.3 Outline of thesis**

This chapter (Chapter 1) is an introduction to the thesis work, and the objectives of

research are described. To have a fundamental understanding of membrane permeation, the principles of different membrane processes are presented in Chapter 2. The mass transport mechanisms involved in the membrane processes are reviewed, and polymers used as membrane materials for various membrane processes are introduced. The resistance model is introduced as well, and it can be used to measure the significance of membrane fouling. Among the several membrane processes, nanofiltration and membrane distillation were found to be the most promising for caprolactam separation from water. As a result, most efforts in this research were spent on these two processes. Chapters 3 and 4 deal with caprolactam removal from water using nanofiltration and membrane distillation. The general conclusions drawn from this study are presented in Chapter 5, where recommendations for future work are also provided.

## **Chapter 2 Literature review**

This literature review mainly covers the basic principles of membrane separation techniques, including membrane transport models and polymer materials used for membranes. Additionally, for liquid separation, the problems of membrane fouling are sometimes significant, and therefore the evaluation of membrane contamination and membrane cleaning are also addressed in this chapter.

### **2.1 Overview of membrane separation technology**

As a rapidly emerging technology, membrane separation has been used in a wide range of applications, from food processing to petrochemical industries. Despite the differences among the various membrane processes, there is one point in common that the membrane, is a semi-permeable barrier that can pass certain components while restricting others under the driving force of a concentration, pressure, temperature or electric potential gradient across the membrane. This process is shown schematically in Figure 2.1.

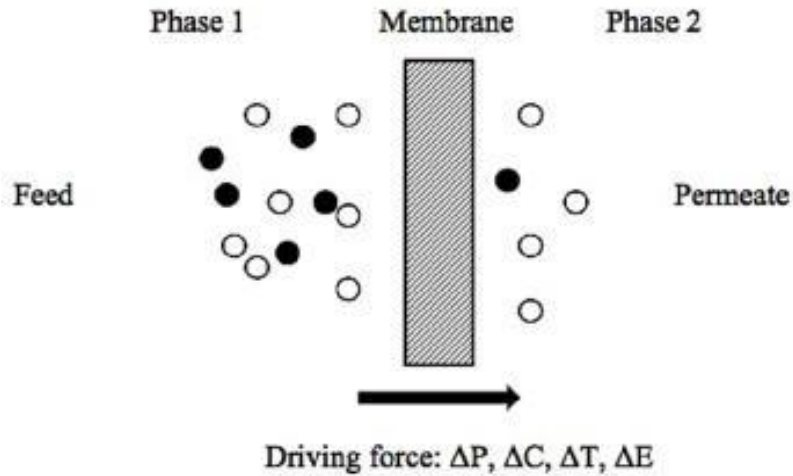


Figure 2.1 Schematic of a two-phase system separated by membrane (Mulder, 1991)

Generally speaking, membranes can be made from either polymeric or ceramic materials. Based on geometry, structure, preparation method and separation manner, membranes can be categorized accordingly (Pinnau and Freeman, 1999), as shown in Figure 2.2.

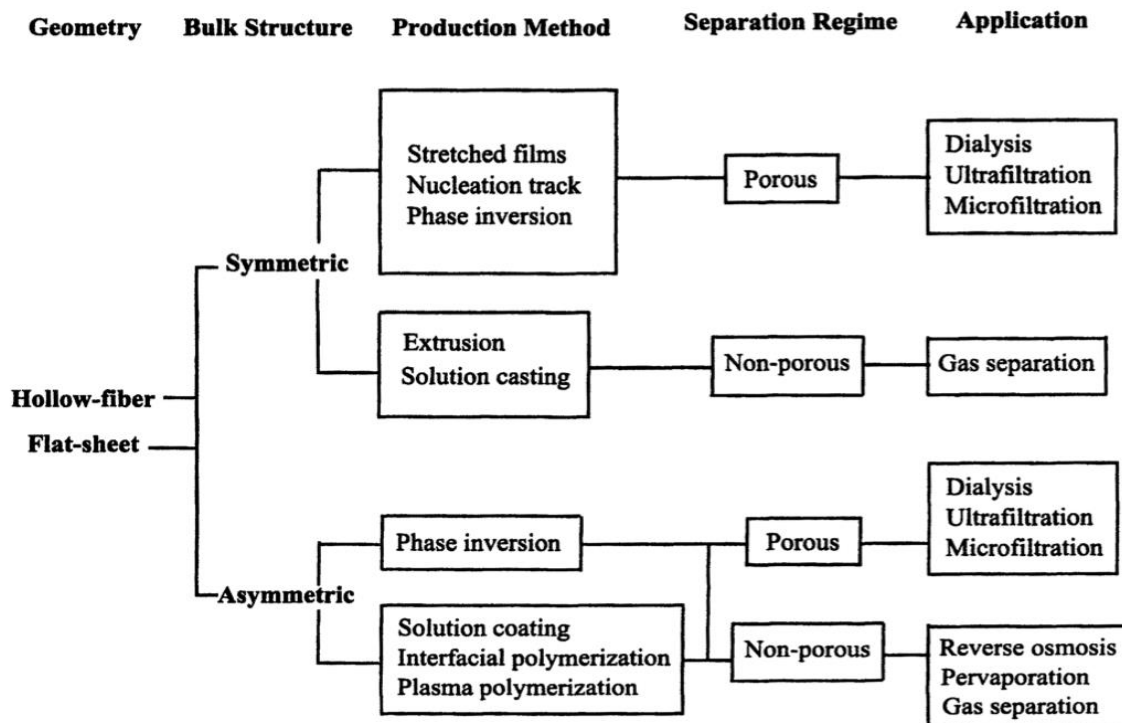


Figure 2.2 Categorizations of synthetic membranes (Pinnau and Freeman, 1999)

Based on their geometries, membranes can be in either flat-sheet or tubular (including hollow fiber) configurations. Flat-sheet membranes are used in plate-and-frame or spiral wound modules, while tubular membranes and hollow fibers normally use modules similar to a tube-and-shell heat exchangers. Flat-sheet membranes are easy to clean and replace, while hollow fiber modules have a high membrane surface area per volume. Both spiral wound and hollow fiber modules are widely used in large-scale industrial applications, whereas plate-and-frame modules are used in certain specific applications (Beasley and Penn, 1981; Baker, 1991).

Furthermore, membranes can be symmetric or asymmetric, and the membrane structure and morphology often determine the separation regime. Symmetric membranes have a typical thicknesses of 10-200  $\mu\text{m}$ , and a uniform structure. For these membranes, the mass transport resistance through the membrane is proportional to the thickness of the membrane. On the other hand, an asymmetric membrane consists of a thin skin layer with a thickness of 0.1-0.5  $\mu\text{m}$  and a porous support layer with a thickness of 50-150  $\mu\text{m}$ . Thus, a high selectivity and a high permeance can be obtained because the membrane resistance is mainly determined by the thin top skin of the asymmetric membrane (Mulder, 1991). Figure 2.3 illustrates the various structures of symmetric and asymmetric membranes.

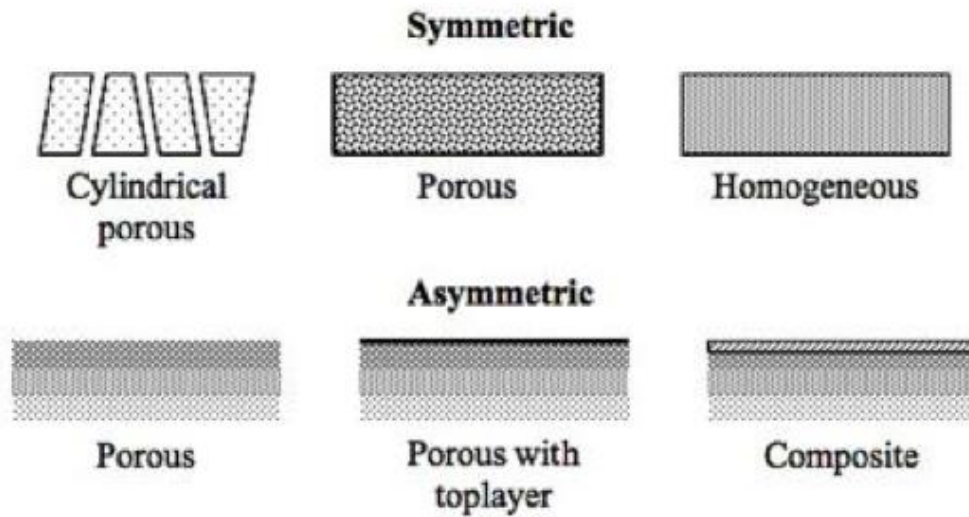


Figure 2.3 Schematic of membrane cross-sections (Mulder, 1991)

Among the well-established membrane processes are microfiltration (MF), ultrafiltration (UF), reverse osmosis (RO), electrodialysis (ED) and dialysis, while such membrane processes as gas separation (GS), pervaporation (PV) and membrane distillation (MD) are developing processes (Mulder, 1991). Pervaporation, nanofiltration and membrane distillation are most relevant to the current study and so are discussed in more details in the following.

### 2.1.1 Pervaporation

Pervaporation is a membrane process during which a liquid feed is maintained at atmospheric pressure, while the permeate stream is removed from the downstream side as a low pressure vapor. The low permeate pressure can be achieved by applying a vacuum pump or using a carrier gas to remove the permeate vapor. Pervaporation separation is based on the difference in diffusivity and solubility of different components of liquid. A



schematic diagram of the pervaporation process is shown in Figure 2.4.

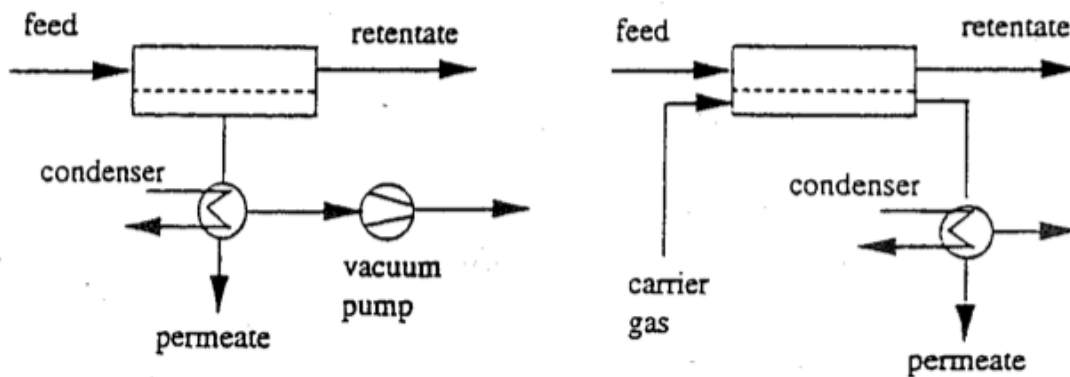


Figure 2.4 Schematic of pervaporation process (Mulder, 1991)

Compared with other energy-intensive separation processes involving phase changes such as distillation, pervaporation is much more energy-effective because the minor components (normally less than 10wt%) in the feed is allowed to permeate through the membrane, and the membrane usually should have a strong affinity to the permeating components, resulting in a high selectivity. Thus, only the minor components in the feed that are preferentially permeable in the membrane consume the latent heat, and therefore pervaporation for separation of azeotropic or close-boiling mixtures is particularly promising. To date, pervaporation is commonly used for dehydration of organic solvents (e.g., alcohols, ethers, esters, acids), removal of dilute organic compounds from aqueous streams (e.g., removal of volatile organic compounds, recovery of aromas) and separation of organic-organic mixtures (Feng and Huang, 1997; Shao and Huang, 2007).

Nonporous membranes are normally required for pervaporation, and three issues should be considered for successful use of pervaporation: membrane productivity,

membrane selectivity and membrane stability (Feng and Huang, 1997). Generally speaking, membranes commonly used in pervaporation are made from polymers or zeolites (Holmes et al., 2000; Bowen et al., 2004).

### 2.1.2 Nanofiltration

Four pressure-driven membrane processes are commonly used to concentrate or purify aqueous solutions: microfiltration, ultrafiltration, nanofiltration and reverse osmosis, depending on the pore sizes of the membranes. The pore sizes, operating pressures and applications of typical pressure-driven membrane processes are summarized in Table 2.1.

Table 2.1 Typical properties of pressure-driven membranes (Shirazi et al., 2010)

Membrane Type	Pore size (nm)	Operating pressure (kPa)	Application
Microfiltration	50-2000	10-50	Separates particles and bacteria from other smaller solutes
Ultrafiltration	2-50	50-200	Separates colloids from solutes such as sugar or salts
Nanofiltration	<2 or non-porous	200-1000	Separates multivalent salts, pesticides, herbicides, etc., from water
Reverse Osmosis	Non-porous	1000-10000	Separates monovalent salts, small molecules and solvents, etc., from water

Nanofiltration (NF) is a pressure-driven filtration process using a membrane with a pore size ranging between those used for reverse osmosis (RO) and those for

ultrafiltration (UF). It is mainly used in water treatment, including production of drinking water and treatment of wastewater (Lau and Ismail, 2009). With a nominal pore size of 1 nm and a transmembrane pressure up to 4MPa, nanofiltration has the advantages of high flux, high rejection of multivalent salts, and low operating and maintenance costs (Hilal et al., 2004).

The selectivity and permeability of pressure-driven membrane processes depend significantly on the membrane pore properties: pore size, pore-size distribution and porosity (Wilderer, 2011). As mentioned before, microfiltration and ultrafiltration membranes are porous and are normally used for low-pressure operations. Meanwhile, reverse osmosis membranes are considered to be nonporous. Nanofiltration membranes fill in the gap between a tight ultrafiltration membrane and a loose reverse osmosis membrane. The molecular weight cut off (MWCO) of a nanofiltration membrane, defined as the molecular weight of the solute that achieves a 90% rejection by membrane, is typically in the range of 100–1000 Da (Schäfer et al., 2005; Oatley et al., 2012).

### **2.1.3 Membrane distillation**

Membrane Distillation (MD) is a membrane separation process in which only vapor molecules can permeate a non-wettable porous membrane. The driving force for mass transport in membrane distillation is the vapor pressure difference across the membrane induced by temperature difference or by applying a vacuum on the downstream side (Mulder, 1991).

Membrane distillation can be used for desalination, wastewater treatment and food processing. It has many advantages because of much lower operating temperatures and pressures than conventional distillation processes. In addition, membrane distillation has a high rejection to non-volatile salts when used for water desalination, and the relative large membrane pore size used in membrane distillation results in a high permeation flux (Alkhudhiri et al., 2012).

Among different membrane distillation configurations, vacuum membrane distillation (VMD) usually exhibits a high permeation flux and negligible heat loss by conduction. Figure 2.5 shows the VMD process schematically, with a vacuum pump used in the permeate side to create the driving force for permeation.

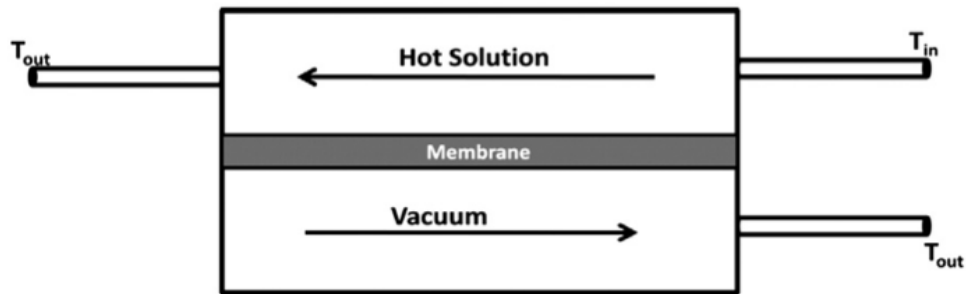


Figure 2.5 Schematic diagram of VMD (Alkhudhiri et al., 2012)

Generally speaking, hydrophobic and microporous membranes are used for desalination of water using membrane distillation. Ideally, the membrane used should have a low resistance to mass transfer, a low thermal conductivity to minimize heat loss across the membrane as well as good thermal and chemical stability. MD membranes are commonly fabricated from such polymers as polytetrafluoroethylene (PTFE),

polypropylene (PP) and poly(vinylidene fluoride) (PVDF) (Sarti, 1993;Pangarkar et al., 2010).

## 2.2 Mass transport mechanism through membranes

As mentioned before, selective mass transfer in the membrane occurs under various driving forces, which may include concentration, temperature, and pressure gradients across the membrane. The ability to control permeation rates of different components is considered as one of the most important properties of membranes. In general, two mass transfer models are used to describe the mechanism of permeation through membranes: the solution-diffusion model and the pore-flow model, as shown in Figure 2.6 (Baker, 2004).

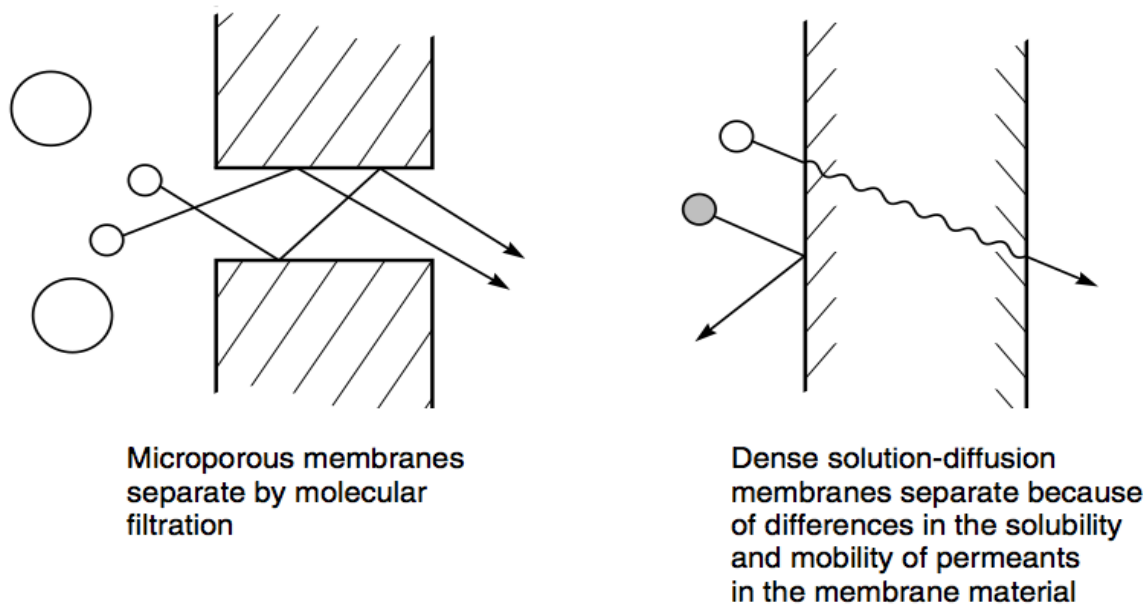


Figure 2.6 Schematic of two types of membrane transport mechanism (Baker, 2004)

Based on the Fick's law of diffusion, the solution-diffusion model describes that the

permeants are separated because of the different solubilities of permeating species in the membrane and their different diffusivities through the membrane. In contrast, the pore-flow model considers that the separation is achieved by size filtration through tiny pores in the membrane, which is applied in many pressure-driven membrane processes (Wijmans and Baker, 1995).

The difference between these two mechanisms lies in the relative sizes and permanence of the pores. For the membrane in which mass transfer is best described by the solution-diffusion model, the free-volume elements (pores) in the membrane are tiny spaces among polymer chains caused by thermal motion of polymer molecules. These free-volume elements fluctuate, and they open and close as permeating molecules pass through the membrane. On the other hand, the pore-flow model is often used to describe membranes in which the pores are fixed, relatively large, and connected to each other (Hwang, 2010). Generally speaking, the transition between solution-diffusion and pore-flow pores is around 5–10 Å diameter.

According to the classification of Baker (2004), membrane transport processes are divided into three groups (Figure 2.7):

1. Transport occurs under pore-flow in membranes in which the pore sizes are larger than 10 Å, and membrane distillation is one of these processes.
2. For polymer chain spaces of less than 5 Å, membranes are considered to have no visible pores, mass transport in such cases is best described by the solution-diffusion model. Pervaporation is a typical process of this group.

3. For membranes with pore diameters of between 5-10 Å, mass transport is somewhere between the pore-flow and solution-diffusion models. Nanofiltration is a typical process of this group.

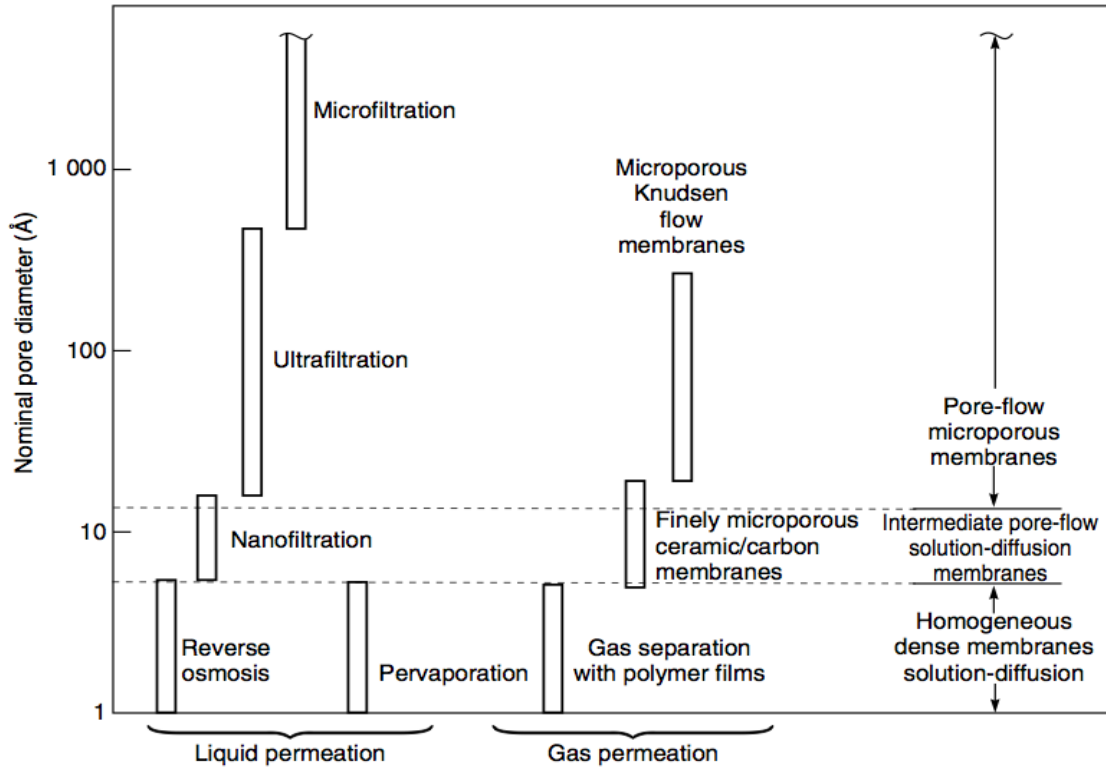


Figure 2.7 Schematic membrane transport models for different membrane processes (Wilderer, 2011)

In this thesis, pervaporation, nanofiltration and membrane distillation were used for caprolactam separation. They will be discussed in details in terms of mass transport in the membranes.

### 2.2.1 Membrane transport in pervaporation

Originally proposed by Graham (Lonsdale, 1982), the solution-diffusion model has been commonly accepted to describe the mass transfer mechanism through dense

membranes. The permeation of molecules through non-porous membranes is considered to consist of three basic steps: 1) the dissolving and sorption of permeant at the feed side interface of a membrane; 2) Diffusion of permeant through the membrane matrix; 3) Desorption of permeant into the downstream side of membrane. In addition, the permeant molecules at downstream side of the membrane during pervaporation are collected in the vapor state, and thus a phase change from liquid to vapor also occurs during the course of permeation.

Assume that equilibrium is reached at the interface between a liquid feed and a membrane in pervaporation. The equilibrium can be expressed as follows:

$$\frac{C_m}{C_{feed}} = K \quad (2.1)$$

where  $C_m$  and  $C_{feed}$  represent concentrations of permeant on the membrane surface and inside the feed, respectively, and  $K$  is the partition coefficient of the permeant between the membrane and feed phases. Sometimes,  $K$  is also called the sorption coefficient.

Among the three steps of the solution-diffusion model, diffusion is the rate-limiting step, which is generally described by the Fick's law:

$$J = -D \frac{dC_m}{dx} \quad (2.2)$$

where  $J$  is the permeation flux,  $dC/dx$  is the concentration gradient, and  $D$  is the diffusion coefficient of the permeant in the membrane. Assuming  $K$  and  $D$  as constants, integrating Eqn. 2.2 and using Eqn. 2.1 gives:

$$J = DK \frac{\Delta C}{L} \quad (2.3)$$

where  $\Delta C$  is the permeant concentration difference across the membrane, and  $L$  is the



thickness of the membrane. The permeability coefficient of the membrane can be defined as:

$$P = DK = \frac{J}{\Delta C} L \quad (2.4)$$

Additionally, to describe the intrinsic mass transport ability of membrane, the permeance,  $Q$ , which is equal to permeation flux normalized by the driving force over the membrane, can be expressed as:

$$Q = \frac{J}{\Delta P} \quad (2.5)$$

Experimentally, the permeation flux,  $J$ , and separation factor,  $\alpha$ , are used to measure the permeability and selectivity of membranes in pervaporation:

$$J = \frac{N}{A\Delta t} \quad (2.6)$$

$$\alpha_{ij} = \frac{P_i}{P_j} = \left(\frac{D_i}{D_j}\right)\left(\frac{K_i}{K_j}\right) = \frac{(Y_i/Y_j)}{(X_i/X_j)} \quad (2.7)$$

where  $N$  is the permeate quantity (gram or mol) collected for the given duration  $\Delta t$  through the membrane with an effective membrane area of  $A$ . The ratios  $D_i/D_j$  and  $K_i/K_j$  are the diffusivity selectivity and solubility selectivity for components  $i$  and  $j$  in the feed mixture, respectively, and  $X$  and  $Y$  are mole fractions of the components in the feed and the permeate side, respectively. Based on Eqn. 2.7, the overall separation factor of membrane  $\alpha_{ij}$ , which represents the preference of one species to another in the feed, is determined by the diffusivity selectivity and solubility selectivity together.

However, a clarification should be made here: The solution-diffusion model described above is the simplest one and only applicable for situations of permeation through non-swollen membranes (Blume et al., 1990). In fact, during pervaporation

operations, membrane swelling and plasticization phenomena may occur. In this case, the interactions among polymer chains decrease and subsequently increase the free volume of the membrane. Consequently, both the solubility coefficient,  $K$ , and diffusivity coefficient,  $D$ , depend on the concentration of penetrants in the membrane. As a result, the classic solution-diffusion model with constant diffusivity and solubility is not applicable for this situation.

### **2.2.2 Membrane transport in nanofiltration**

NF membranes have pore sizes in the range between those of tight ultrafiltration membranes and loose reverse osmosis membranes. Consequently, the mass transport mechanism through NF membranes may be described as a combination of solution-diffusion and pore-flow mechanisms (Schäfer et al., 2005).

However, the NF transport process is not yet well understood. Tremendous efforts have been made to build mass transfer models that can describe NF processes for separation of different salts or organics. Among these, theories based on the extended Nernst-Planck model (ENP) (Bowen and Mukhtar, 1996) and the Spiegler and Kedem model (SP) (Ismail and Hassan, 2004) are accepted by most researchers. In addition, the Teorem-Meyer-Siever (TMS) and the Donnan-Steric pore model (DSPM), and certain other models are also used (Wang et al., 1995; Ismail and Hassan, 2006).

### **2.2.3 Membrane transport in membrane distillation**

The pore-flow model has been popular until the mid-1940s. This model considered that the separation was achieved because certain components in the feed excluded by the pores of the membrane while other components were able to penetrate based on molecule sieving effect. This model is well applied in the membrane distillation process in which microporous membranes are commonly used.

Several parameters are used to characterize microporous membranes, including the membrane porosity,  $\varepsilon$ , which stands for the porous fraction of the total membrane volume, the membrane tortuosity,  $\tau$ , which represents the ratio of the average pore length over the membrane thickness, and the diameters of pores in a membrane,  $d$  (Baker, 2004).

For gas or vapor permeation in microporous membrane, depending on collisions between molecules or between molecules and a wall of pores in a membrane, the mechanisms of mass transport through microporous membranes will be different. Knudsen diffusion takes place when the pore size of a membrane is much smaller than the mean free path of the permeating molecules because the molecule-molecule interactions are insignificant compared to the collisions between molecules and the membrane. If the molecule-molecule collisions are dominant over the interactions between permeating molecules and the membrane when a membrane has large pore sizes, the Poiseuille flow will apply. The mean free path  $\lambda$  is defined as the average distance travelled by molecules to make collisions:

$$\lambda = \frac{k_B T}{\sqrt{2\pi P} d_e^2} \quad (2.8)$$

where  $k_B$  is the Boltzman constant,  $T$  and  $P$  are the absolute temperature and average pressure inside the membrane pores, respectively, and  $d_e$  is the diameter of the permeating molecule, which is assumed to be a hard sphere (Alkudhiri et al., 2012). The ratio of  $\lambda$  to the membrane pore size  $r$  is normally called Knudsen number  $K_n$ .

When  $K_n > 20$ , the Knudsen flow model applies for mass transport through a membrane (Bandini and Sarti, 1999), and the molar permeation rate  $N_i$  is expressed as:

$$N_i = \frac{2\pi}{3} \frac{1}{RT} \left( \frac{8RT}{\pi M_{wi}} \right)^{\frac{1}{2}} \frac{r^3}{\tau L} \Delta P_i \quad (2.9)$$

where  $M_{wi}$  is the molecular weight of permeating component  $i$ , and  $\Delta P_i$  is transmembrane pressure of component  $i$ .

When  $0.02 < K_n < 20$ , the mass transfer is controlled by both the Knudsen and Poisseille model, and can be described as (Banat and Simandl, 1994):

$$N_i = \frac{\pi}{RTL\tau} \left[ \frac{2}{3} \left( \frac{8RT}{\pi M_{wi}} \right)^{\frac{1}{2}} r^3 + \frac{r^4}{8\mu} P_{avg} \right] \Delta P_i \quad (2.10)$$

where  $\mu$  is the viscosity of the species, and  $P_{avg}$  is the average pressure in the pore.

When  $K_n < 0.02$ , the mass transfer through the membrane can be described by the Poisseille flow and expressed as (Khayet and Matsuura, 2004):

$$N_i = \frac{\pi r^4}{8\mu} \frac{P_{avg}}{RT} \frac{1}{\tau L} \Delta P_i \quad (2.11)$$

### 2.3 Polymers used as membrane materials

Membranes are prepared from both organic and inorganic materials. One major part of these materials is polymer. To prepare a specific membrane, the selection of proper

polymer materials is based on both specific properties and structural features of the polymers.

Either completely coiled or uncoiled, polymers can be either homopolymers with all the same repeating segments or copolymers in which the repeating units of the polymer are different. The structure of a polymer can be either linear or branched. Two or more chains can also be connected to each other by means of crosslinks (Mulder, 1991).

The state of a polymer can be glassy or rubbery. The glass transition temperature  $T_g$  is defined as the state at which a polymer changes from glassy to rubbery. Most physical properties of polymers change at  $T_g$ , including permeability, refractive index and free volume. The free volume, defined as the fraction of the volume not occupied by the macromolecules, influences the properties of polymers significantly (Bernardo et al., 2009). There exists a relatively large free volume in rubbery polymers, resulting in a high permeability in these polymers. Polymers in the glassy state tend to have a high selectivity, good mechanical stability and low permeability because as the fractional free volume decreases, so does the space for large-scale movement of penetrants through the polymers.

The degree of crystallinity is another significant parameter influencing the mechanical and transport properties of polymers. Most polymers are semi-crystalline, consisting of both crystalline and amorphous segments. The permeability in a crystalline region is low due to the extended tortuosity of penetration paths, and the mass transport of penetrants takes place mostly in amorphous regions (George and Thomas, 2001). For

semi-crystalline polymers, the amorphous glassy state transforms into a rubbery state under the glass transition temperature,  $T_g$ . The crystalline region is more stable until the melting temperature  $T_m$  is reached, transforming them from a glassy to a rubbery state (Mulder, 1991).

The membranes used in the current study for the caprolactam removal from wastewater by pervaporation, nanofiltration and membrane distillation are all polymer based membranes. They will be discussed below in more details.

### 2.3.1 Polyamides

Polyamide is a polymer with repeating units linked by amide bonds ( $-CO - NH -$ ). Due to its excellent chemical stability, thermal stability and permselectivity, polyamide is commonly used as a membrane material in pressure-driven and pervaporation membrane separation processes.

Table 2.2 Physical properties of nylon 6 (Brandrup, 1999)

Property	Value
Density ( $\text{g/cm}^3$ )	1.08
$T_g$ (°C) Glass transition temperature	50
$T_m$ (°C) Melting point	220
Water adsorption at equilibrium (%)	$9.5 \pm 0.5$
Tensile strength (MPa)	78

Formed by ring-opening polymerization of caprolactam, polyamide 6 (nylon 6) is a semi-crystalline, thermoplastic polyamide with excellent strength, which makes it promising as a membrane material (Mallick and Khatua, 2011). Nylon 6 was developed by Schlack to reproduce the properties of nylon 6,6 without infringing the patent on its production, and nylon 6 has been extensively used in various industries. Typical properties of nylon 6 are listed in Table 2.2 (Brandrup, 1999).

Various attempts have been made to prepare membranes from modified nylon 6. For example, nylon 6-graft-poly(hexyl methacrylate) and nylon 6-graft-poly(ethyl methacrylate) are used for making membranes for pervaporation separation of benzene/cyclohexane mixtures (Yoshikawa and Tsubouchi, 1999). Nylon 6-graft-polyoxyethylene membranes are also used for pervaporation of cyclohexane/cyclohexanone/cyclohexanol mixtures (Okushita et al., 1996). Theoretically, nylon 6 is supposed to have an excellent affinity with caprolactam, which is the monomer of nylon 6. Therefore the preparation of nylon 6 membranes for pervaporation separation of caprolactam from water was attempted in the present thesis work.

Besides pervaporation, polyamides are also widely used for pressure-driven membrane separation processes. Polyamide was first used in the 1960s when DuPont and Monsanto developed asymmetric, integrally skinned hollow fibers for reverse osmosis (RO) seawater desalination (Schäfer et al., 2005). To keep within the scope of this thesis study, this section focuses only on polyamides that are used in nanofiltration processes, since large quantities of thin film composite NF membranes have been developed from

interfacially polymerized polyamides that act as thin active layers on porous supports made of polymers such as polysulfone (PSf) or polyethersulfone (PES) (Song et al., 2005).

Many studies have discussed TFC-NF membranes prepared by the interfacial polymerization technique. The thin polyamide layer is formed by reaction between two active monomers, i.e. a polyfunctional amine and a polyfunctional acyl chloride at the interface of two immiscible solvents. Using interfacial polymerization, (Song et al., 2005) produced different TFC-NF membranes formed from trimesoyl chloride (TMC) and p-phenylenediamine (PPD), m-phenylenediamine (MPD) and piperazine (PIP), respectively, on polysulfone (PSf)/sulfonated polysulfone (SPSf) substrates. Another TFC-NF membrane was formed using polyethyleneimine (PEI) and TMC (Fang et al., 2013). A schematic of the interfacial polymerization process and possible reaction mechanism for PEI/TMC membrane formation are presented in Figures 2.8 and 2.9, respectively.

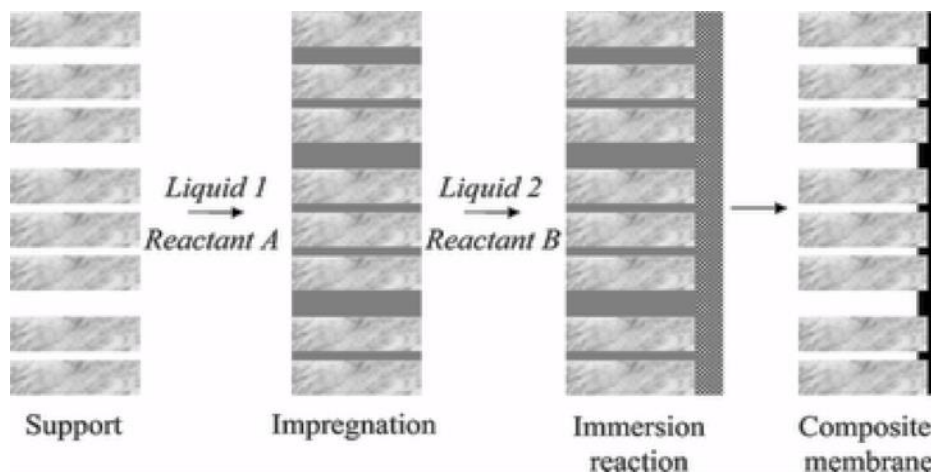


Figure 2.8 Interfacial polymerization for membrane formation



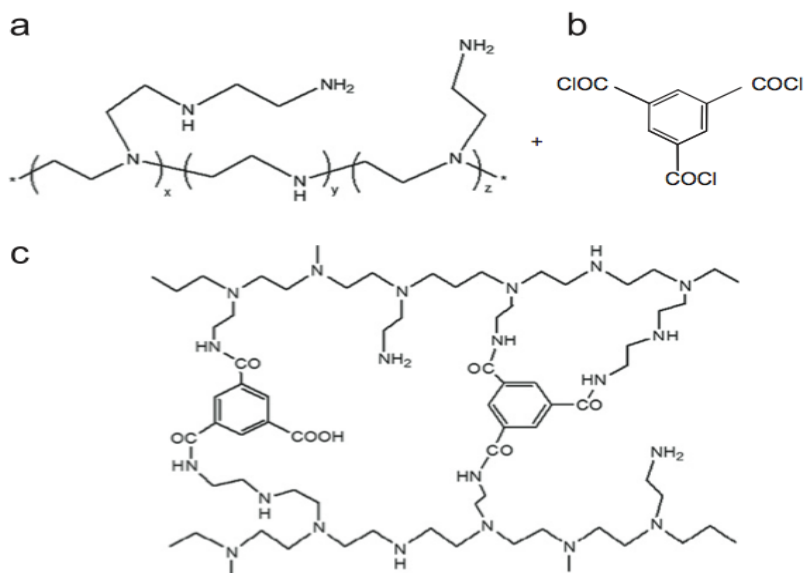


Figure 2.9 Polyamide formation between PEI and TMC (Fang et al., 2013)

### 2.3.2 Polytetrafluoroethylene (PTFE)

As a synthetic fluoropolymer of tetrafluoroethylene, PTFE is highly crystalline and hydrophobic. Therefore, neither water nor other water-containing substance can wet PTFE. It has been used widely due to its strong carbon–fluorine bonds, which makes PTFE chemically stable and non-reactive. Consequently, it is used commonly in containers or pipework for reactive and corrosive chemicals (Mulder, 1991; Sun and Zhang, 1993). The best known brand name of PTFE is Teflon, produced by DuPont. Some physical properties of DuPont™ PTFE are listed in Table 2.3.

Table 2.3 Physical properties of DuPont™ PTFE (Dupont, 2006)

Property	Value
Density (g/cm <sup>3</sup> )	2.2
T <sub>m</sub> (°C) Melting point	327
Water adsorption at equilibrium (%)	<0.01
Tensile strength (MPa)	21-23
Hardness (HB)	50-65

For thermally driven membrane distillation (MD), the membranes should have a low resistance to mass transfer and a low thermal conductivity to prevent heat loss through the membrane. During the MD process, it is important for the membrane not be wetted. The wettability of liquids on membrane materials can be explained by the Laplace equation (Franken et al., 1987) as:

$$\Delta P = -\frac{2\gamma_i}{r} \cos\theta \quad (2.12)$$

where  $\Delta P$  is the transmembrane pressure across the membrane,  $\gamma_i$  is the surface tension,  $r$  is the pore size of the membrane, and  $\theta$  is the contact angle of a liquid on membrane materials.

Based on Eqn. 2.12, to prevent wetting, the maximum size of pores in a membrane used for MD should be 0.1-0.6 $\mu$ m (Schneider et al., 1988). The surface tension of the liquid mainly lies in the structure of liquid molecules as well as the intermolecular forces such as weak polar forces or strong hydrogen bonding. Table 2.4 summarized the surface tensions of a few liquids:

Table 2.4 Surface tension of some liquids at 20°C (William et al., 2012)

<b>Liquids</b>	<b>Surface tension <math>\gamma_i</math> (<math>10^3</math> N/m)</b>
Water	72.8
Methanol	22.6
Ethanol	22.8
Glycerol	63.4
Formamide	58.2
N-hexane	18.4

A higher surface energy results in easier wetting. Table 2.5 summarizes the surface energy of selected polymers (Van Krevelen, 1972). It can be seen from Table 2.5, PTFE has the lowest surface energy, which exhibits the highest hydrophobicity. In fact, membranes made from polytetrafluoroethylene (PTFE), polypropylene (PP) or polyvinylidene fluoride (PVDF) are all commonly used for MD.

For vacuum membrane distillation, the driving force for mass transport is provided by lowering the permeate pressure below the saturated vapor pressure. Though the heat loss through the membrane is not as significant as in thermally driven membrane distillation, it is important to prevent the liquid from entering the membrane pores under the transmembrane pressure created by the vacuum pump on the permeate side.

Table 2.5 Surface energies of some polymers (Van Krevelen, 1972)

<b>Polymer</b>	<b>Surface energy <math>\gamma_s</math> (<math>10^3</math> N/m)</b>
Polytetrafluoroethylene	19.1
Polytrifluoroethylene	23.9
Polyvinylidene fluoride	30.3
Polyvinylchloride	36.7
Polyethylene	33.2
Polypropylene	30.0
Polystyrene	42.0

## **2.4 Membrane contamination**

### **2.4.1 Fouling and concentration polarization**

During the membrane separation processes, membrane performance is often inevitably affected by membrane contamination, which is usually reflected in flux decline and deterioration of membrane selectivity over time. Membrane contamination is one of the most significant problems in membrane processes. Surface fouling of membrane is the most severe problem of membrane contamination.

Membrane fouling can result from several factors such as concentration polarization, cake layer formation, membrane pore blocking and adsorption of solute molecules on membrane surface. Each of these factors results in additional resistance to mass transport across the membrane. Figure 2.10 illustrates the major resistances acting in porous membrane (Shirazi et al., 2010). Overall, membrane fouling is a complex physicochemical phenomenon in which several mechanisms are involved simultaneously

(Hilal et al., 2005).

Concentration polarization on membrane surface should be distinguished from membrane fouling, although membrane fouling can result initially from concentration polarization. Imagine a membrane separation process in which the solvent permeates across membrane but the solute is partly rejected. Over time, the retained solutes gradually accumulate on the surface of the membrane, and the concentration gradient of the solutes build up in the boundary layer until a steady state is reached. Consequently, the convective solute flow from the liquid bulk to membrane surface is balanced between the diffusive flow from the membrane surface back to solution bulk ( $-D \frac{dC}{dx}$ ) and the permeate flow across the membrane ( $J.C_p$ ). This relationship can be expressed in Eqn. 2.13, and a schematic of the concentration profile in the boundary layer is shown in Figure 2.11 (Mulder, 1991).

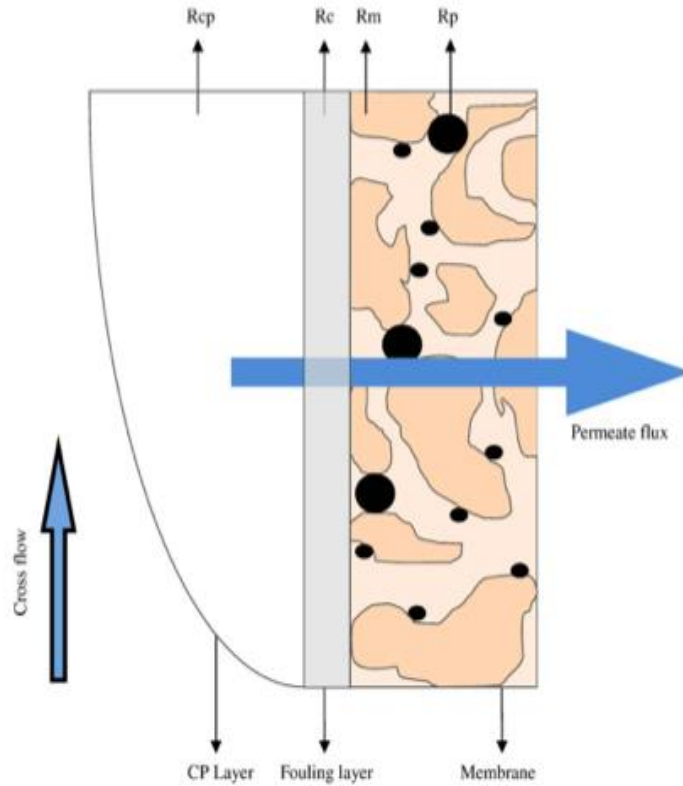


Figure 2.10 Major mass transfer resistances in porous membranes.  $R_{cp}$ ,  $R_c$ ,  $R_m$  and  $R_p$  represent resistance due to concentration polarization, cake layer formation, the membrane and pore-blocking, respectively (Shirazi et al., 2010).

$$J \cdot C = J \cdot C_p - D \cdot \frac{dC}{dx} \quad (2.13)$$

The boundary conditions are:

When  $x = 0$ ,  $C = C_m$

When  $x = \delta$ ,  $C = C_b$

where  $\delta$  is the thickness of the boundary layer,  $C_m$  and  $C_b$  are solute concentrations at the membrane surface and in the bulk solution, respectively.  $D$  is the solute diffusivity in the boundary layer, and  $J$  is the solute permeation flux.

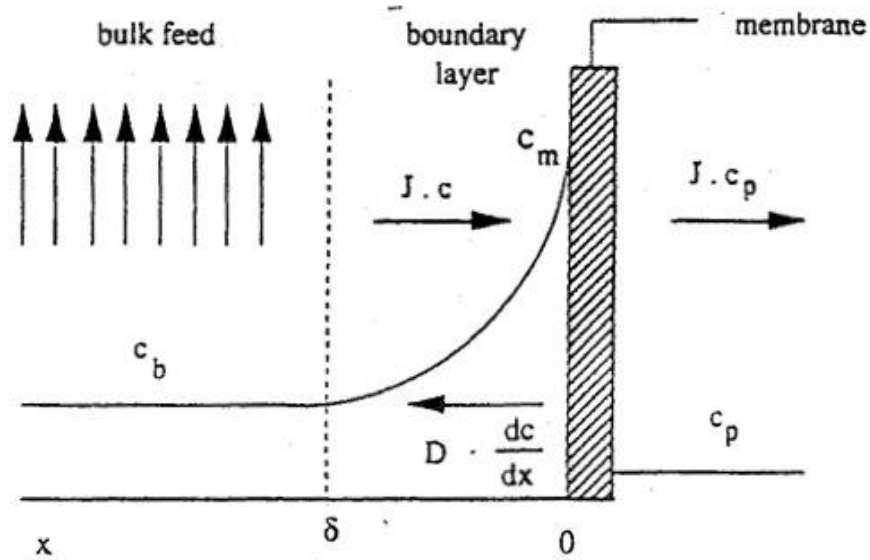


Figure 2.11 Concentration profile build-up in boundary layer (Mulder, 1991)

Integrating Eqn. 2.13 gives:

$$\ln \frac{c_m - c_p}{c_b - c_p} = \frac{J\delta}{D} \quad \text{or} \quad \frac{c_m - c_p}{c_b - c_p} = \exp\left(\frac{J\delta}{D}\right) \quad (2.14)$$

defining the mass transfer coefficient  $k$  as the ratio of the diffusion coefficient  $D$  over the boundary layer thickness  $\delta$ :

$$k = \frac{D}{\delta} \quad (2.15)$$

if the intrinsic retention ( $R_{int}$ ) of the membrane can be defined as:

$$R_{int} = 1 - \frac{c_p}{c_m} \quad (2.16)$$

then Eqn. 2.14 can be re-arranged to give

$$\frac{c_m}{c_b} = \frac{\exp\left(\frac{J}{k}\right)}{R_{int} + (1 - R_{int})\exp\left(\frac{J}{k}\right)} \quad (2.17)$$

where the ratio  $(c_m/c_b)$  is known as the concentration polarization modulus. According to Eqn. 2.17, increasing flux  $J$  and membrane retention  $R_{int}$  or decreasing the mass transfer coefficient  $k$  can lead to a high concentration polarization modulus, in other

words, more severe concentration polarization.

Generally, concentration polarization has negative effects on permeation flux, and the significance of concentration polarization differs for different membrane processes. For instance, the pressure-driven processes, including microfiltration and ultrafiltration, are affected significantly by concentration polarization. On the other hand, separation processes with dense membrane such as gas separation are influenced much less significantly by concentration polarization because of the high diffusivity of molecules in gas phase.

#### **2.4.2 Resistance-in-series model**

As mentioned before, the fouling problem and concentration polarization are influenced by membranes used, permeate solutions, and operating conditions (e.g. feed concentration, transmembrane pressure (TMP)). In addition to the resistance of the membrane itself ( $R_m$ ), concentration polarization, internal pore blocking and gel-layer formation will yield additional mass transfer resistances (i.e.,  $R_{cp}$ ,  $R_{in}$  and  $R_g$ , respectively). In order to understand the fouling behavior during membrane separation processes, the resistance-in-series model is often used to evaluate the resistances of each components (Tu et al., 2005;Kaya et al., 2011). Generally, the relationship between permeate flux and resistance can be described as follows:

$$J = \frac{\Delta P}{\mu R_{tot}} = \frac{\Delta P}{\mu(R_m + R_g + R_{cp} + R_{in})} \quad (2.18)$$

where  $\Delta P$  is the transmembrane pressure, and  $\mu$  is the viscosity of the permeate



solution.

when pure water permeates a membrane, the flux relationship is given by:

$$J = \frac{\Delta P}{\mu R_m} \quad (2.19)$$

As a result, the membrane resistance  $R_m$  can be obtained from pure water permeation data. Using the membrane resistance  $R_m$  calculated, the fouling resistance  $R_f$  can also be calculated from the solution permeation data of solution based on Eqn.2.18. The typical flux-pressure relationship for pure water and a solution permeation are shown in Figure 2.12.

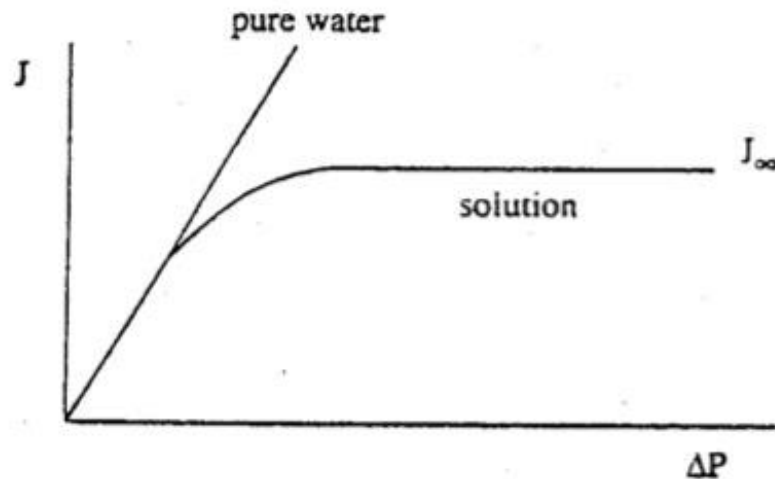


Figure 2.12 Flux-applied pressure curves for pure water and a solution permeation (Baker, 1991)

The difference in fouling behavior between a surface and internal pore of a membrane is distinct in that membrane surface fouling is reversible in most cases, but the internal fouling due to pore blocking is partly irreversible, and the membrane performance cannot be recovered completely by washing. (Arora et al., 2009).

### **2.4.3 Methods employed for fouling control**

There are different methods for controlling membrane fouling, based on specific membranes and separation applications (Hilal et al., 2005):

#### **1. Pretreatment of feed solution**

Pretreatment of the feed solution is often used, especially in pervaporation and membrane distillation where fouling is not severe. This approach is commonly used to remove and filter particles that may cause pore blocking of a membrane or to prevent particles and macromolecules from depositing on the membrane surface. Generally, pre-filtration, PH pre-adjustment and chemical clarification are commonly used as pretreatment (Peuchot and Aim, 1992).

#### **2. Modification of membrane materials**

Modification of membrane properties is an attractive approach to reduce adhesive fouling by changing surface properties while keeping the macroporous structure of membranes. Membrane properties such as hydrophilicity/hydrophobicity, narrow pore size distribution or charged surface (in applications involving charged colloids) can all help reduce adhesive fouling. Methods to modify membrane properties include surface coating with a polymer layer having antifouling properties and grafting, to immobilize hydrophilic species onto the membrane from solutions (Iwata et al., 1991; Nunes et al., 1995).

#### **3. Optimization of operating conditions**

Fouling effect can also be reduced by improvement of operating parameters, especially flow conditions. Methods such as increasing the feed flow rate, introduction of turbulence promoters, etc., are also normally used (Winzeler and Belfort, 1993).

#### 4. Cleaning

Among all the fouling control approaches, membrane cleaning is used most frequently. Depending on the chemical foulants and resistance of the membranes, three cleaning methods can be used: hydraulic cleaning, mechanical cleaning, and chemical cleaning. Through back-flushing, changing feed flow direction at a given frequency or alternate pressuring, hydraulic cleaning is commonly applied in cross-flow filtration processes, while mechanical cleaning is often used in tubular systems. Chemical cleaning with a number of chemicals (e.g., acids, alkali, enzymes, detergent or complexing agents like EDTA) is the most significant cleaning method in fouling control (Mulder, 1991).

### **2.5 Removal of caprolactam from wastewater by membranes**

Separation and reuse of caprolactam from wastewater generated during caprolactam production is significant from both an economic and environmental points of view. Tremendous efforts have been made on caprolactam separation from wastewater. Currently, the recovery of caprolactam from its aqueous solution is primarily done using extraction with an organic solvent (e.g., benzene, toluene, ether, esters and ketones) followed by back-extraction with water (Xie et al., 2002; Van Delden et al., 2006). Additionally, works have also been done to treat such caprolactam-containing wastewater

by biological degradation of caprolactam. e.g., Kulkarni (1998) reported the bioremediation of caprolactam from wastewater by use of *Pseudomonas aeruginosa* MCM B-407, which is a microorganism isolated from activated sludge (Kulkarni and Kanekar, 1998). Another caprolactam-degrading bacteria, *Alcaligenes faecalis*, used by Baxi (2002), is also an example for bioremediation of wastewater containing caprolactam (Baxi and Shah, 2002).

However, the organic solvents used to extract caprolactam from wastewater such as benzene and toluene are usually toxic, flammable and volatile, while bioremediation of caprolactam-containing wastewater is not efficient enough to decompose all the caprolactam without recycling and recovery in the economic point of view. Compared to these two processes above, membrane separation techniques are clean (without introduction of pollutants), energy-saving and possible to separate caprolactam from wastewater for reuse as well.

Unfortunately, very little work has been reported in the literature on caprolactam separation from wastewater by membranes. This study attempts to explore the various membrane processes for such an application in order to identify appropriate membrane processes that can be used for caprolactam separation. This exploratory research will look into nanofiltration, pervaporation and membrane distillation for possible use in caprolactam separation. The research findings are of interest from both an application and academic point of view in consideration of the lack of relevant information in the literature.

## **Chapter 3 Experimental**

This study looks into three membrane processes: nanofiltration, pervaporation and membrane distillation for potential use in removal of caprolactam from wastewater. The general operation procedures and experimental setups of the three membrane processes are presented in this chapter, where the membranes used during these processes are also introduced.

### **3.1 Nanofiltration**

Theoretically, with a molecular weight cut off (MWCO) 100–1000 Da, nanofiltration (NF) is thought to be a suitable process for removal of caprolactam from water. Therefore the separation performance of NF processes to separate caprolactam from water was evaluated at different operating conditions (e.g., pressure and feed concentration). One potential problem with nanofiltration is membrane fouling. Thus, NF experiments were conducted with not only caprolactam solution but also pure water permeation to evaluate membranes fouling resistances in NF based on the resistance-in-series model.

#### **3.1.1 Membranes**

Five nanofiltration membranes were studied for caprolactam separation from water. Two membranes were synthesized in the lab by interfacial polymerization of

polyethyleneimine (PEI) and trimesoyl chloride (TMC) on top of a polyethersulfone substrate (PES-10, supplied by Sepro Membranes). The PES support was washed thoroughly with de-ionized water overnight to remove preservatives and dried in air. PEI and TMC were dissolved in water and hexane, respectively, which would be used for interfacial polymerization between the aqueous and the organic phase. The concentration of PEI and TMC in the aqueous and organic solutions was 3.5 and 0.7 wt%, respectively. The PES substrate was allowed to contact with the aqueous PEI reactant for 45 mins at ambient temperature, followed by contact with the organic TMC reactant solution for 30 mins, thereby inducing interfacial reaction between PEI and TMC to form a thin-film-composite membrane. This membrane was designated as Membrane 1. Similarly, the PES substrate was also allowed to contact the organic reactant first, followed with contact with the aqueous reactant, and such membrane was designated as Membrane 2.

In addition, 3 commercial NF membranes (NF1 and NF 2 membranes from Sepro Membranes, Filmtech NF45 membrane from Dow Chemical) were also tested.

### **3.1.2 Nanofiltration experiments**

NF tests were carried out in a stirred nanofiltration cell of 250ml capacity; the NF membrane was cut into proper size and installed inside. The effective area of membrane in the cell was  $12.56 \text{ cm}^2$ , and the stirring speed was controlled by a magnetic stirrer, as shown in Figure 3.1. The permeation cell was pressured with nitrogen gas to provide the

transmembrane pressure for permeation. The feed pressure, ranging from 0 to 0.8 MPa, was measured by a pressure gauge.

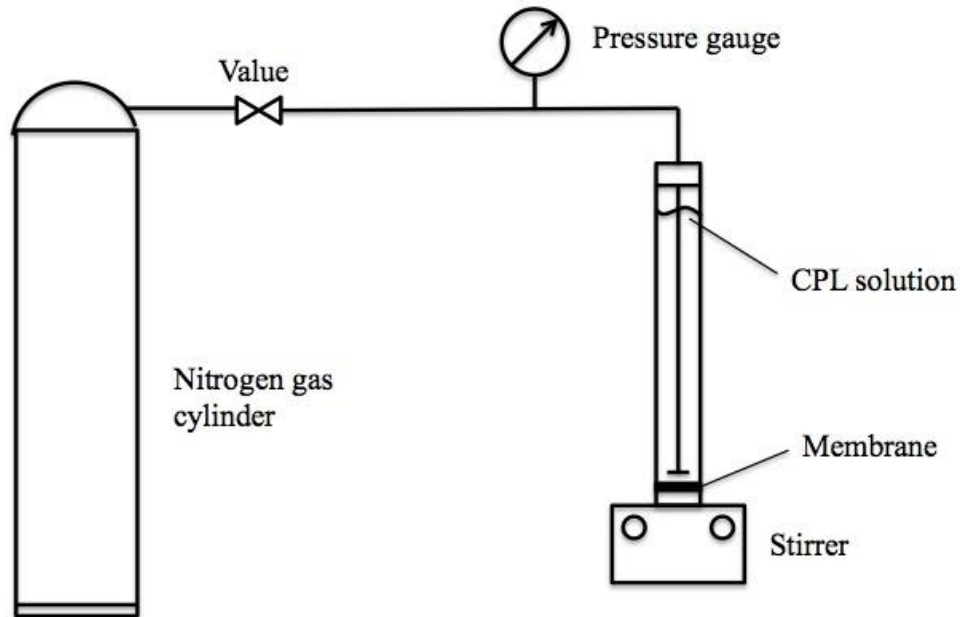


Figure 3.1 Schematic of nanofiltration setup

Each new NF membrane placed inside the cell was preconditioned by permeation of 250 ml pure water under 0.8MPa before NF tests with the caprolactam solution. The amount of permeate collected from the downstream side of membrane was weighed by a digital balance, and the concentrations of caprolactam in the feed and permeate were measured by a refractometer. The permeate flux was calculated from the permeate collected over a given period of time and the membrane area:

$$J = \frac{N}{A\Delta t} \quad (3.1)$$

where the N is the quantity of permeate collected over a given duration  $\Delta t$  through the

membrane with effective membrane area A.

The caprolactam rejection was calculated from caprolactam concentrations in feed and permeate:

$$R = \left(1 - \frac{C_p}{C_f}\right) \times 100\% \quad (3.2)$$

Where  $C_p$  and  $C_f$  represent the permeate and feed caprolactam concentration (wt%) respectively.

In order to study the effect of operating parameters (e.g., pressure and feed concentration) on the NF performance, NF membranes were tested with caprolactam concentrations in the feed ranging from 0-5wt% under a feed pressure of 0.1-0.8MPa. During the experiments, the feed pressure was first increased from 0.1 to 0.8MPa then decreased to ensure that the membrane was not compacted under pressure and the reproducibility of the permeability and rejection data.

In addition, a NF membrane was selected for batch operation to test the variation of “dead end” NF performance over time.

### **3.2 Pervaporation**

In view that caprolactam is the precursor of nylon 6, nylon 6 is expected to have strong affinity with caprolactam. Pervaporation is based on selective solubility and diffusivity of a permeant in the membrane, and very often the solubility aspect dominates permeability. There have been cases where bigger molecules can permeate through a



membrane faster than a smaller permeant as long as the membrane has sufficient affinity to the preferentially permeating molecules. Thus, nylon 6 membranes were prepared in the lab for tests in caprolactam separation from water by pervaporation. If caprolactam could permeate through the nylon 6 membrane, it would be of significant interest because caprolactam is the minor component to be removed from water.

Pervaporation (PV) was performed with nylon 6 membrane prepared in lab to test the permeability and separation factor for caprolactam removal from water. Nylon 6 was supplied by Sigama-Aldrich Co., and nylon 6 membrane was prepared as follows: nylon 6 was dissolved in formic acid for 24 h to form a homogeneous solution containing 15wt% nylon 6. Then the solution cast onto a glass plate with a preset thickness, followed by drying in a dust-free chamber at room temperature. Finally, the membrane was vacuum-dried at room temperature for 6 h to remove any residual solvent.

The membrane cell used in pervaporation process was similar to that described in Figure 3.1. The difference was that the pervaporation cell was equipped with a jacketed feed reservoir, and a thermal bath circulator was used to control and adjust the operating temperature (Haake-Fisons Instruments Inc.), as shown in Figure 3.2. The downstream side of membrane was connected to a vacuum pump with a vacuum gauge and two cold traps for collection of permeate sample. The cold traps were submerged in liquid nitrogen to condense permeate collected.

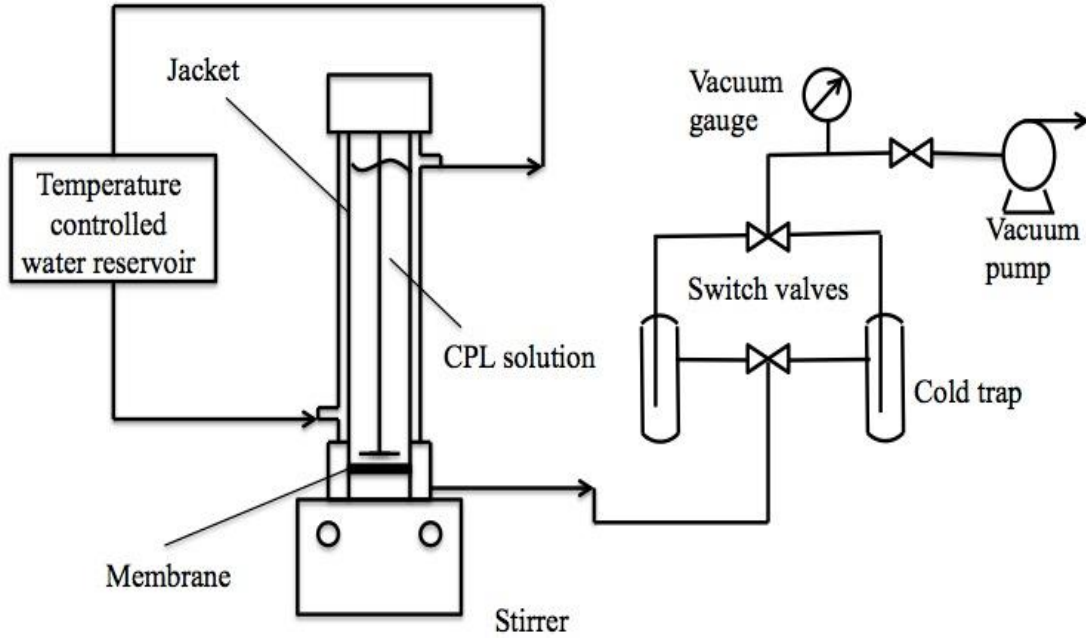


Figure 3.2 Schematic of pervaporation apparatus

In pervaporation, the permeate flux and separation factor were used to characterize the permeability and selectivity of membrane respectively. The permeation flux  $J$  was determined in the same way as in nanofiltration, and the separation factor  $\alpha_{i/j}$  was determined from:

$$\alpha_{i/j} = \frac{\left( \frac{Y_i}{Y_j} \right)}{\left( \frac{X_i}{X_j} \right)} \quad (3.3)$$

where  $X$  and  $Y$  represent the weight fractions of the permeating components in the feed and the permeate, respectively.

### 3.3 Vacuum membrane distillation

Vacuum membrane distillation (VMD) uses a microporous membrane to permeate a volatile component. As water is much more volatile than caprolactam, water vapor molecules will preferentially pass through the pores of the membrane. As a result, hydrophobic microporous membranes should be used to prevent the feed liquid from entering the membrane pores. Therefore, microporous PTFE membranes were chosen to be used for the separation of caprolactam from water by removing water from the feed mixture. It is in fact a concentration process where water is removed from the feed by membrane distillation.

The PTFE membrane with a pore size of  $0.1\mu m$  was supplied by W.L. Gore and Associates, Inc. The experimental setup for vacuum membrane distillation was essentially the same as that used for pervaporation as shown on Figure 3.2. Vacuum was applied on the permeate side of the membrane. The pressure on the permeate side was maintained at  $<2$  kPa absolute throughout the experiments. The permeation flux and permeate concentration were determined. In addition, the contact angle of water on the membrane surface was also measured by a Tanteq contact angle meter in order to characterize the surface properties of the membrane. Material with a water droplet contact angle lower than  $90^\circ$  is normally considered hydrophilic.

As the same to nanofiltration, the permeation flux and caprolactam rejection are also used to characterize the membrane performance during vacuum membrane distillation

process.

## Chapter 4 Results and Discussion

### 4.1 Nanofiltration

#### 4.1.1 Effect of operating conditions on nanofiltration performance

As a pressure-driven membrane process, nanofiltration was conducted at different pressures and feed concentrations. The water permeation flux and caprolactam rejection rate were determined at pressures from 0.1 to 0.8 MPa with a feed caprolactam concentration of 0 to 5wt% at room temperature (about 25 °C) using 5 different nanofiltration membranes. Figures 4.1 to 4.5 show the permeation flux and caprolactam rejection of Membranes 1, 2, NF1, NF2 and NF-45, respectively.

As expected, the permeate flux rises with increasing operating pressure, but it is not always linear relationship. Based on the solution-diffusion model, the water flux through NF membrane follows a linear pattern with applied hydrostatic pressure:

$$J_v = A(\Delta P - \Delta\pi) \quad (3.1)$$

where  $J_v$  is water flux,  $\Delta\pi$  is difference in osmotic pressure and  $A$  is water permeability constant. For pure water permeation, if the membrane resistance is constant, then

$$J = \frac{\Delta P}{\mu R_m} \quad (3.2)$$

where  $\mu$  stands for viscosity of water and  $R_m$  is the resistance of the membrane. In this case, osmotic pressure is no longer relevant for pure water permeation, and the pure water flux is proportional to the applied pressure consequently.

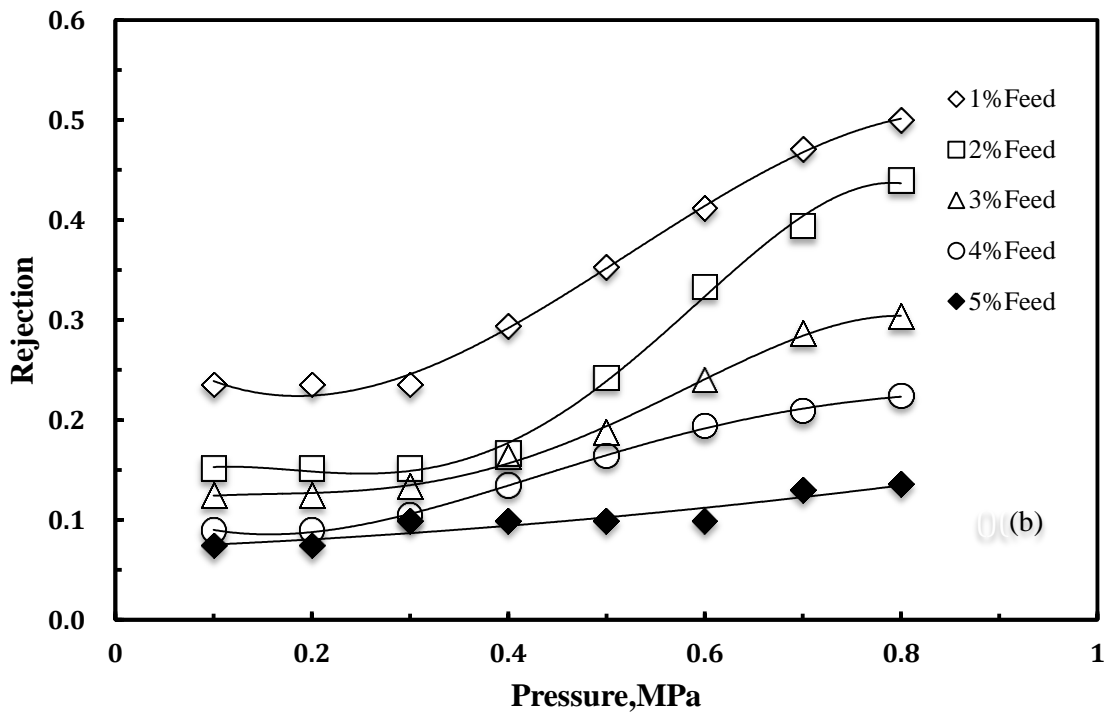
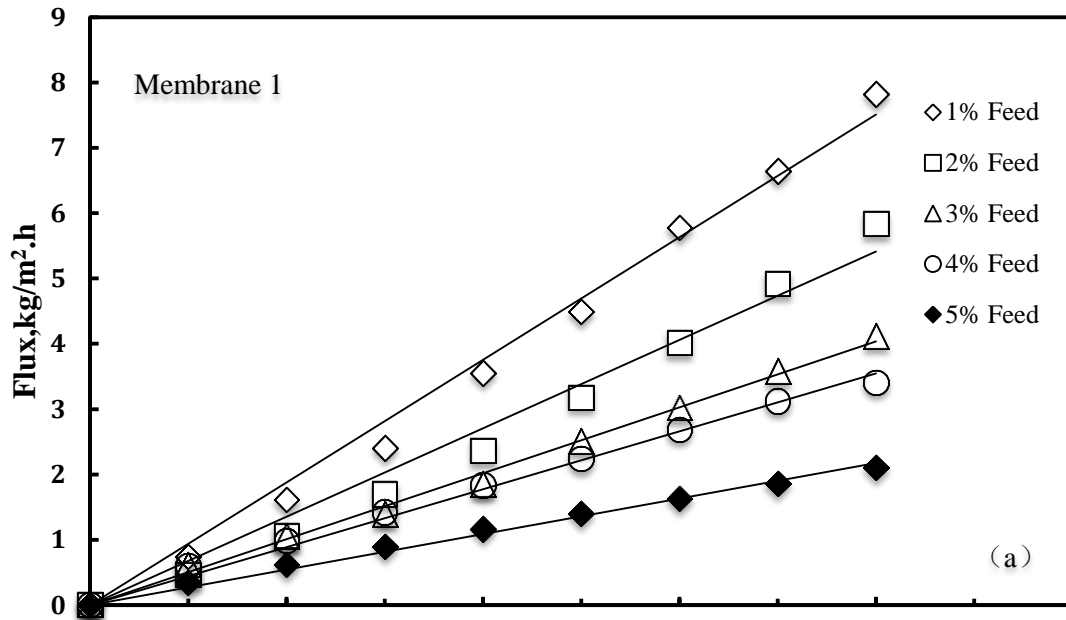


Figure 4.1 Effect of operating pressure on permeation flux (a) and caprolactam rejection (b) at different feed caprolactam concentrations, Membrane 1

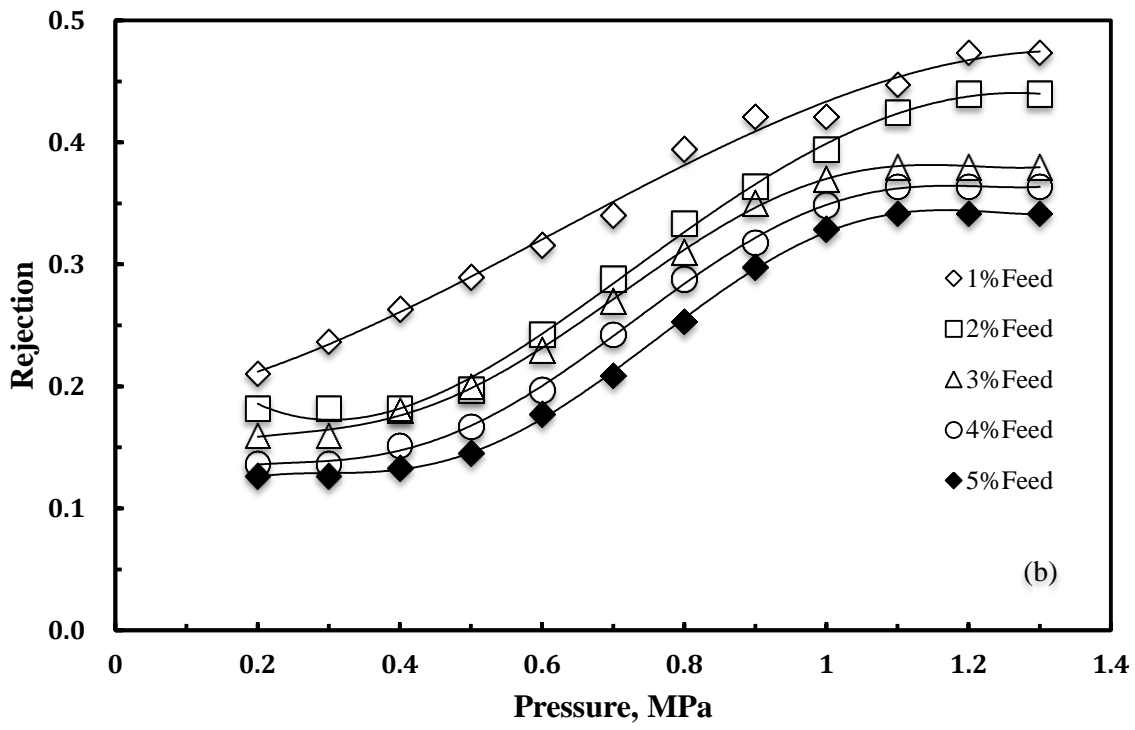
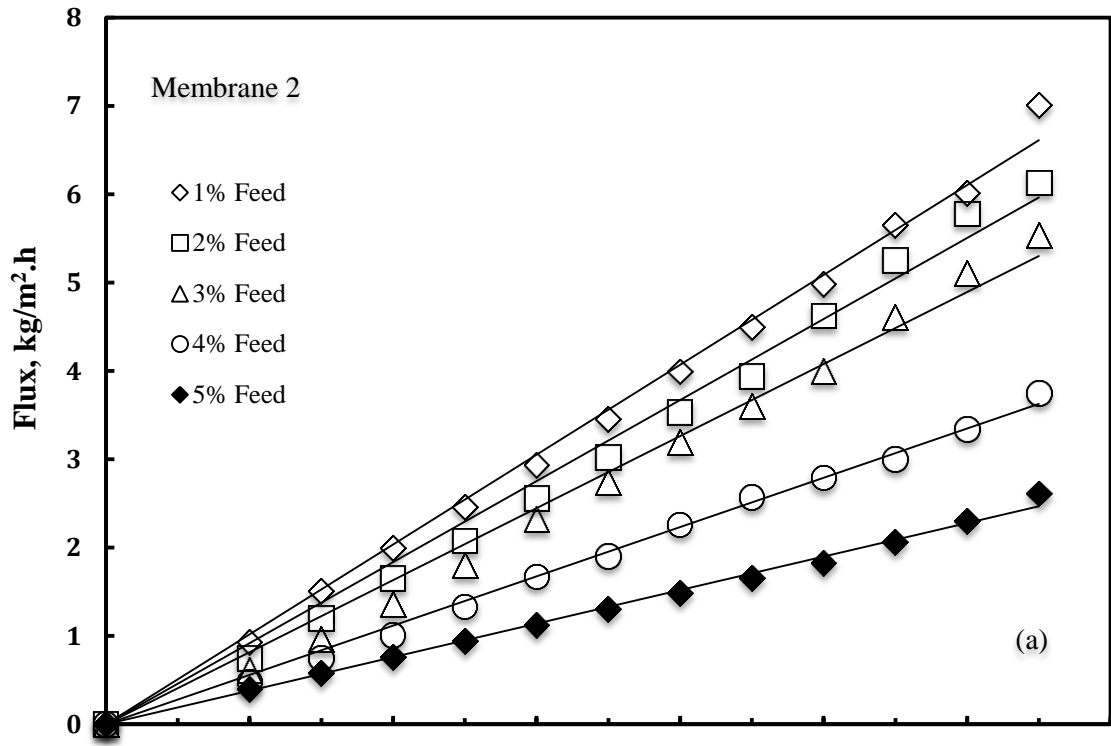


Figure 4.2 Effect of operating pressure on permeation flux (a) and caprolactam rejection (b) at different feed caprolactam concentrations, Membrane 2

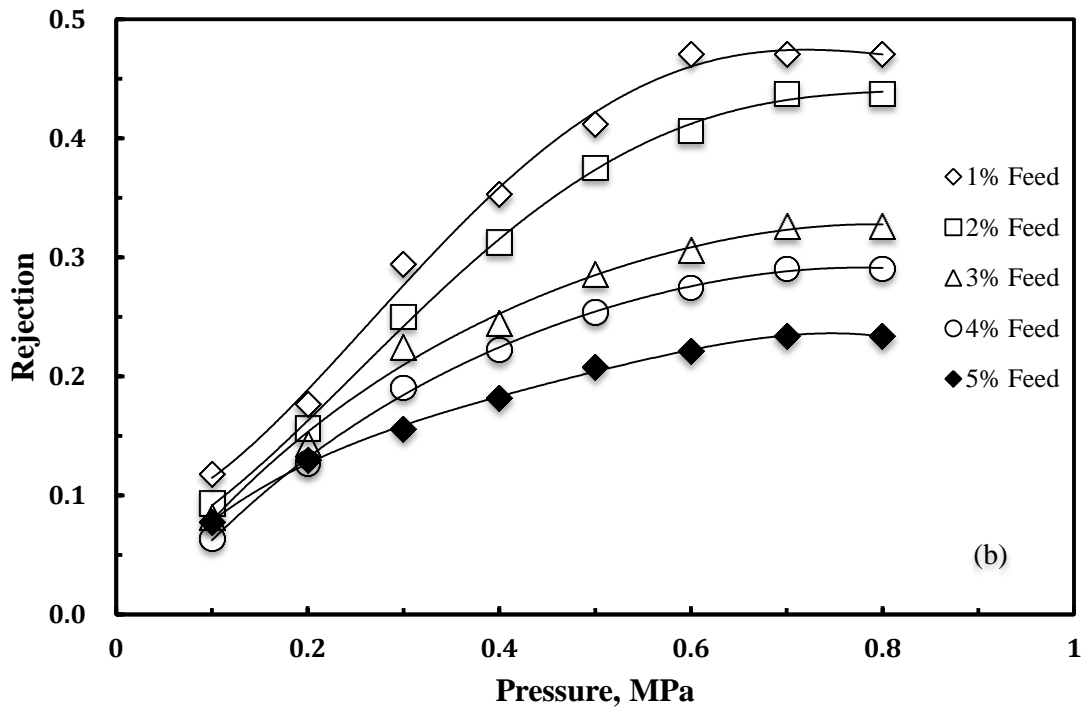
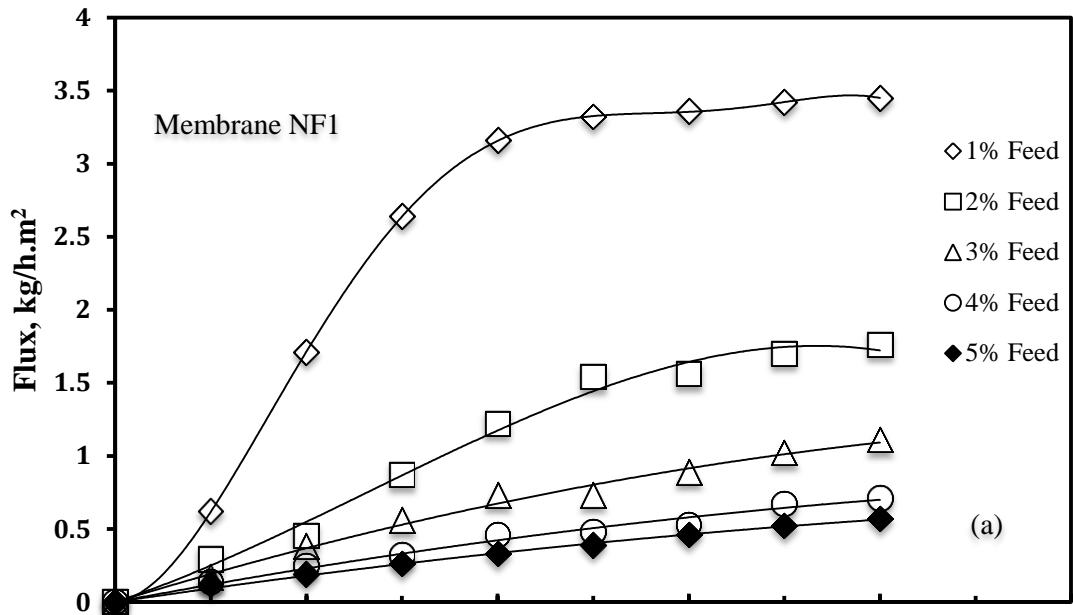


Figure 4.3 Effect of operating pressure on permeation flux (a) and caprolactam rejection (b) at different feed caprolactam concentrations, Membrane NF1



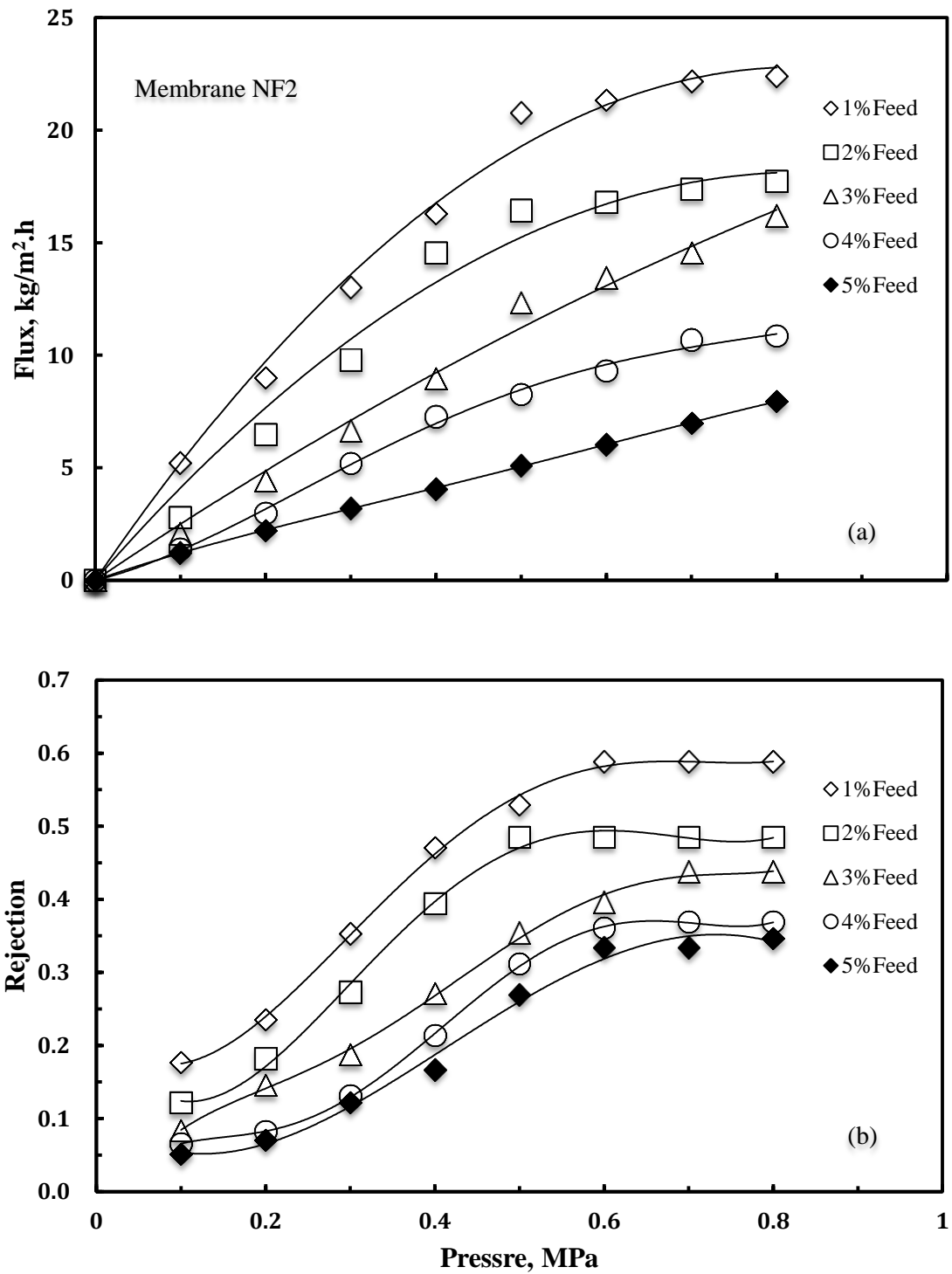


Figure 4.4 Effect of operating pressure on permeation flux (a) and caprolactam rejection (b) at different feed caprolactam concentrations, Membrane NF2

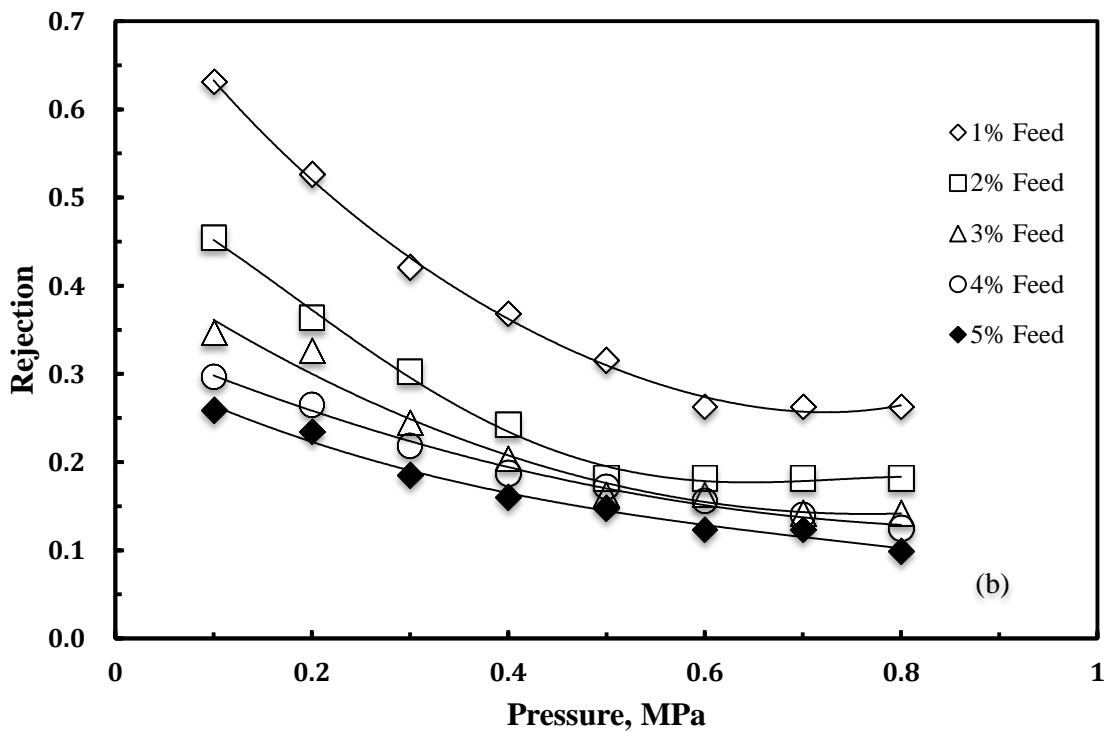
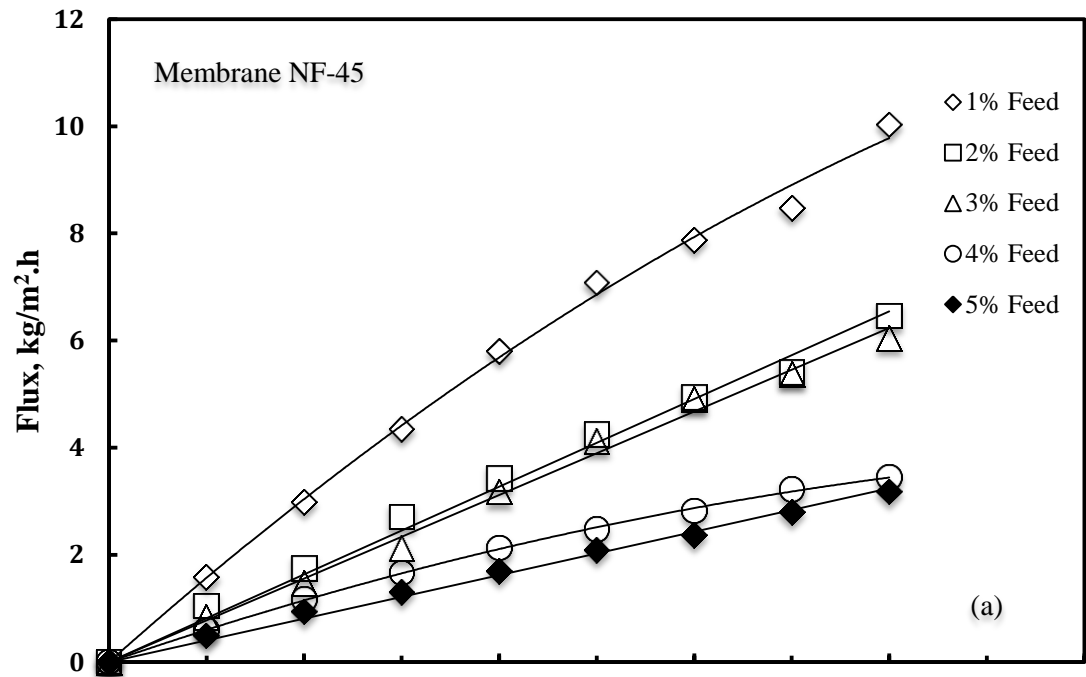


Figure 4.5 Effect of operating pressure on permeation flux (a) and caprolactam rejection (b) at different feed caprolactam concentrations, Membrane NF-45

It can be seen that for Membrane 1 and Membrane 2, the water permeation flux varies with pressure almost linearly. This appears to suggest that concentration polarization during permeation of caprolactam solution through these two membranes are insignificant presumably due to the relatively low caprolactam rejection that results in a small difference in osmotic pressure between feed solution and boundary layer. Similar observations can also be noted in literature for other nanofiltration systems (Mehiguene et al., 1999; Frarès et al., 2005).

At a given feed caprolactam concentration and operating pressure, Membrane 1 is more permeable than through Membrane 2. This may attribute to the different sequence of deposition with the aqueous and organic reactant solutions during interfacial polymerization for membrane preparation. Membrane 1 was formed by depositing PEI macromolecules on PES substrate to react with TMC small molecules at the interface between the aqueous and organic phases, while Membrane 2 was formed by depositing small molecular TMC followed by interfacial polymerization with macromolecular PEI. The deposition of large molecules PEI onto the surface of the porous substrate will result in less densely packed molecules inside the pores of the membrane because macromolecules penetrate the pores less easily than small molecules. Schematic of reactant deposition sequence for membrane formation by interfacial polymerization is shown in Figure 4.6, and the sequence of the reactant deposition onto the microporous substrate is thought to be the main reason for the higher permeability of Membrane 1 than

Membrane 2.

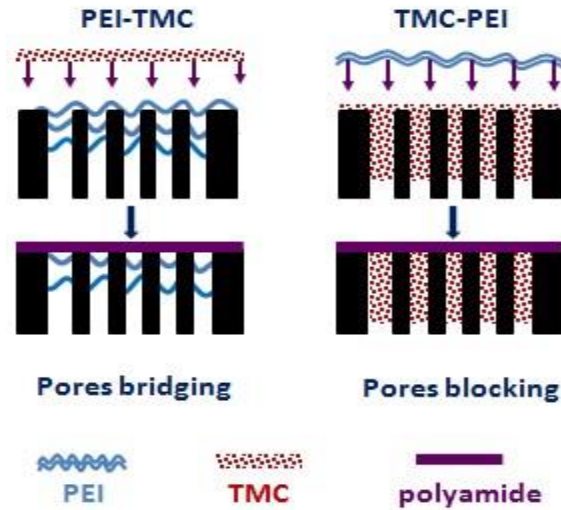


Figure 4.6 Schematic of reactant deposition sequence for membrane formation by interfacial polymerization

Membrane fouling and concentration polarization are often important in nanofiltration. The permeation of caprolactam solution through Membrane NF1, Membrane NF2 and Membrane NF-45 showed a different trend in permeation flux with applied pressure. In this case, the permeation flux also increases almost linearly with increasing applied pressure at relatively low pressures, but the flux does not increase at the same rate with pressure when the pressure is relatively high.

Caprolactam is a neutral organic solute, and it is expected to have a high affinity to polymeric NF membranes, which have amide groups for the interfacially polymerized Membrane 1 and Membrane 2 as well. As filtration process proceeded, the solute concentration became gradually higher near the membrane surface, and the solutes retained by the membrane can attach to and accumulate on the membrane surface easily.

Consequently, an additional mass transport resistance will result, which causes the permeation flux to increase with pressure less than proportionally. This flux-pressure relationship is also seen for other nanofiltration systems (Marín and López-Ramírez, 2011; Fang et al., 2013).

The influence of feed caprolactam concentration on caprolactam rejection at a given pressure can also be observed from figures shown above. For all the 5 membranes studied here, the permeation flux decreases as the feed concentration increases. This may be caused by the higher osmotic pressure and/or higher solution viscosity when the feed concentration increases, which results in a decrease in the permeation flux. In addition, the flux decrease at a higher caprolactam concentration in the feed may also be related to membrane fouling and concentration polarization. Any adsorption of the solute molecules from bulk feed to the surface and/or inner pores of the membrane will tend to reduce the permeation flux.

As far as the caprolactam retention is concerned, Membrane 1, Membrane 2, Membrane NF1 and Membrane NF2 showed similar rejection rate. Generally, it can be said that the rejection of caprolactam increases with operating pressure for a given feed concentration, and when the pressure is sufficiently high, the retention gradually levels off, as shown in Figures 4.1-4.5.

According to Van der Horst, the diffusive transport of solute dominates over convective flow and results in low rejection performance at low operating pressures. (Van der Horst et al., 1995). With an increase in operative pressure, the solvent flux tends to

increase, and increased membrane fouling will enhance the rejection of caprolactam. On the other hand, the concentration polarization will be more severe with increasing pressure as well, which tends to lower the solute rejection values. Consequently, the caprolactam rejection data appear to suggest that the fouling effect is more significant than the concentration polarization, and the net effect results in an increased caprolactam rejection.

Different from the above 4 membranes, the rejection-pressure relationship for Membrane NF-45 is shown to have an opposite trend, that is, the rejection of caprolactam decreases with an increase in the operating pressure. Similar results are also reported in the literature (Frarès et al., 2005). Technically, the rejection decline could be attributed to gradually higher concentration polarization. However, the linear relationship between permeate flux with operating pressure suggests that the concentration polarization is not significant. Thus, concentration polarization cannot be the dominating factor for the decreased caprolactam rejection. On the other hand, Membrane NF-45 is a commercial thin film composite membrane with a very thin skin layer, which is an interfacially formed polyamide matrix, when caprolactam adsorbed onto the surface and inner pores of the membrane, the membrane structure may be altered by caprolactam. In order to verify whether this is the case, pure water permeation was tested with a virgin NF-45 membrane before and after caprolactam solution permeation, and the results are shown in Figure 4.6.

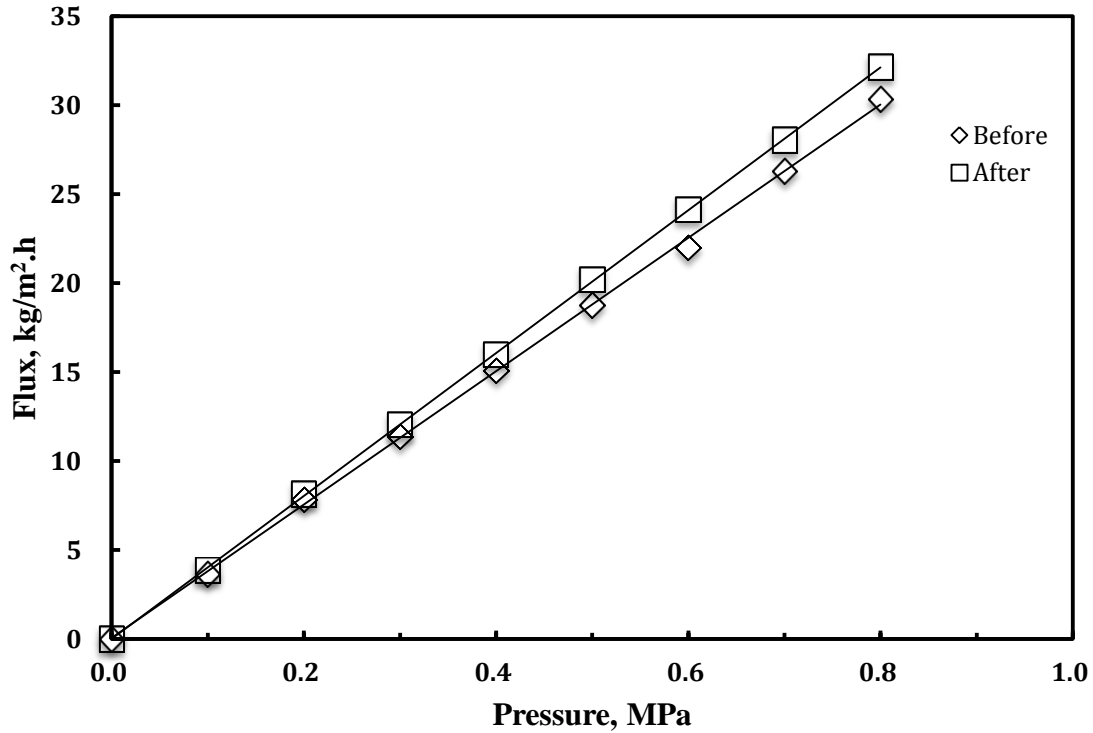


Figure 4.7 Pure water permeation results before and after caprolactam NF test in Membrane NF-45

Clearly, the pure water permeation flux after permeation with aqueous caprolactam solutions became higher than the value before caprolactam NF test, which indicates the membrane has undergone a structural change that makes the membrane more permeable and less selective, resulting in a decrease in the rejection of caprolactam.

Another reason could be that the interactions between the membrane and caprolactam solution would be more facilitated for growth of the streaming force in the pores and makes it stronger than surface force of membrane due to surface properties change, which lowered caprolactam rejection. Similar curve has been reported in other literature (Frarès et al., 2005).

Based on the caprolactam NF results, the caprolactam rejection is shown to be in the

range between 10-60%. This is far from satisfactory, but the NF process can be applied as a pretreatment for perconcentration of caprolactam from wastewater, which can be followed by conventional liquid-liquid extraction or distillation when the caprolactam concentration is high enough.

#### **4.1.2 Fouling Resistance on nanofiltration membranes**

Membrane fouling tends to make the process less productive as far as permeation rate is concerned. During the NF experiments, it had been found that both permeate flux and rejection of caprolactam separation from water were influenced by membrane fouling. It was thus decided to determine the membrane resistance  $R_m$  and resistance caused by membrane fouling  $R_f$  based on the resistance-in-series model.

To calculate Membrane resistance  $R_m$ , the virgin test was conducted for permeation of pure water under different pressures with membranes that had never been used for caprolactam separation previously. The permeate flux is plotted against the operating pressure, which turned out to be a straight line through the origin point, and  $R_m$  was calculated from the slope of the flux-pressure relationship (see Eqn. 3.2).  $R_f$  is calculated for permeation values for a 5% caprolactam feed solution by subtracting the membrane resistance from the total mass transfer resistance. The  $R_m$  and  $R_f$  so determined for the five tested membranes are shown in Figures 4.8 to 4.12.



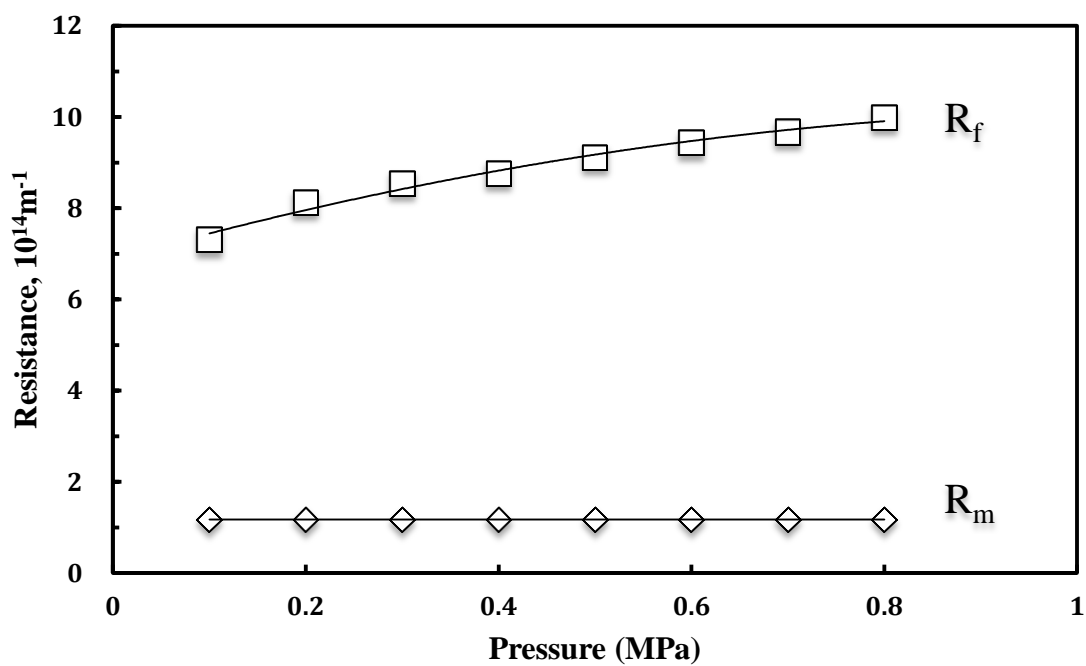


Figure 4.8 Membrane and fouling resistances as a function of pressure, Membrane 1

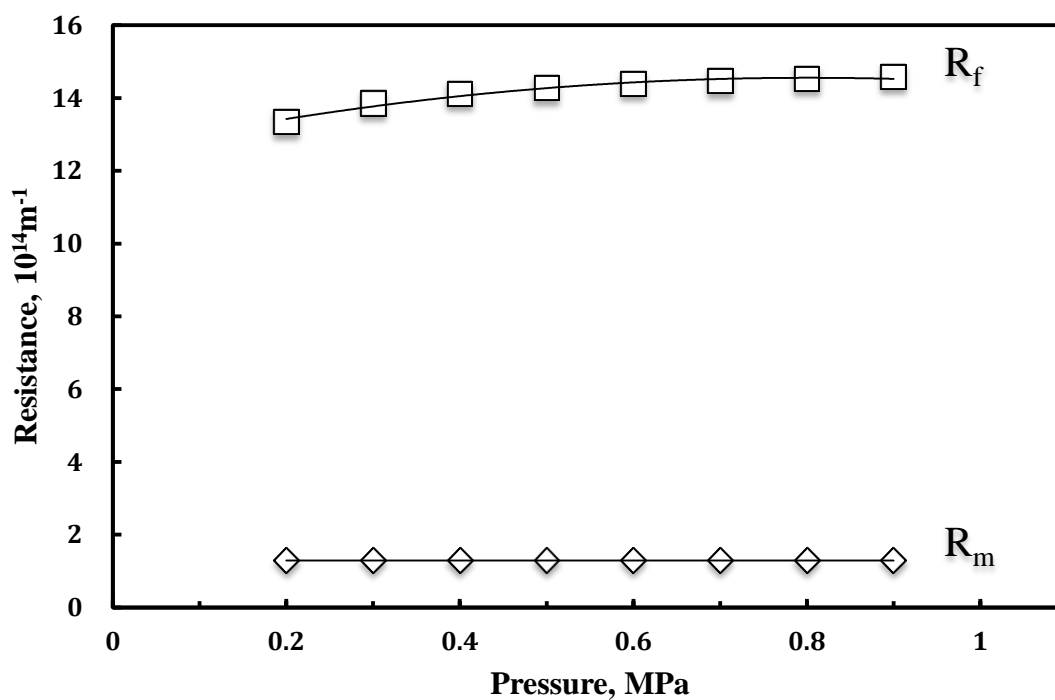


Figure 4.9 Membrane and fouling resistances as a function of pressure, Membrane 2

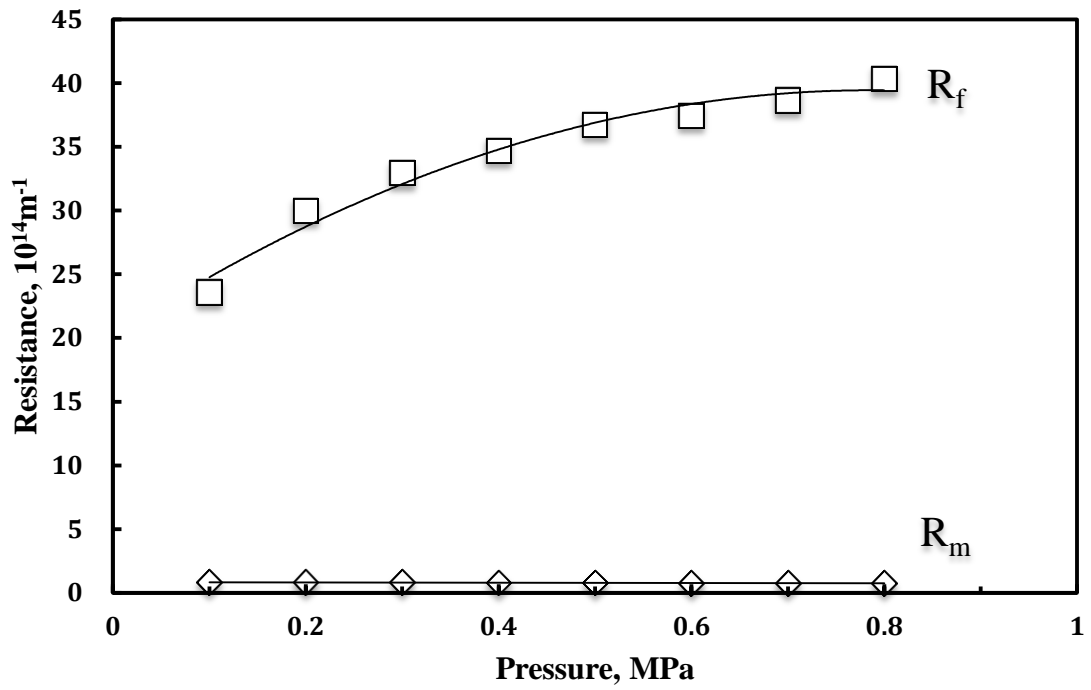


Figure 4.10 Membrane and fouling resistances as a function of pressure, Membrane NF1

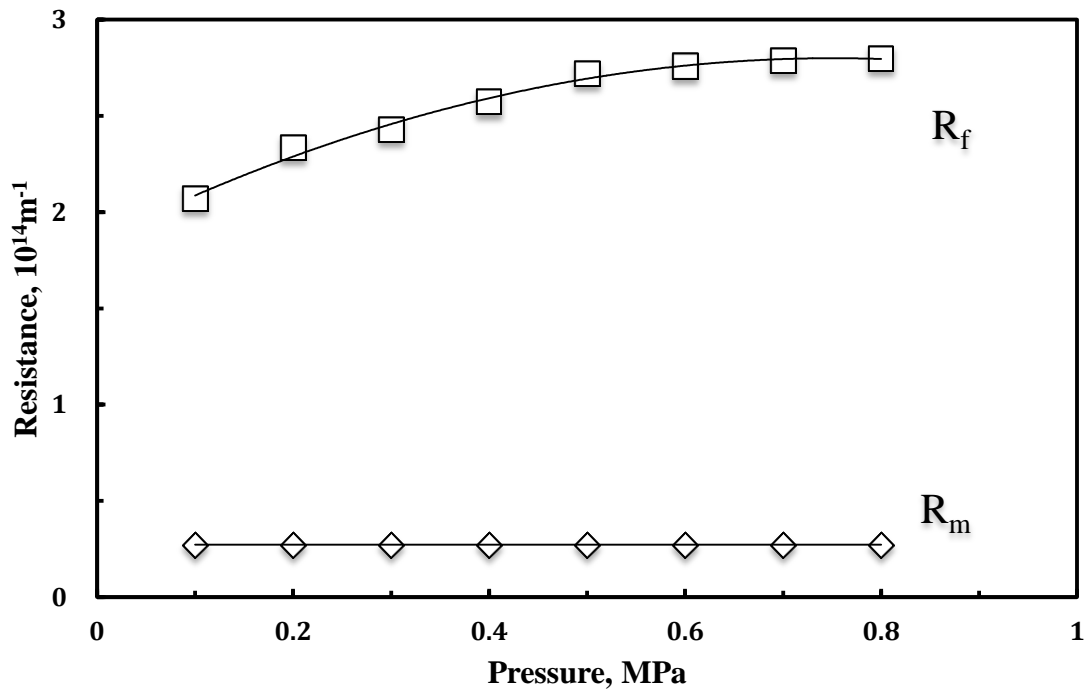


Figure 4.11 Membrane and fouling resistances as a function of pressure, Membrane NF2

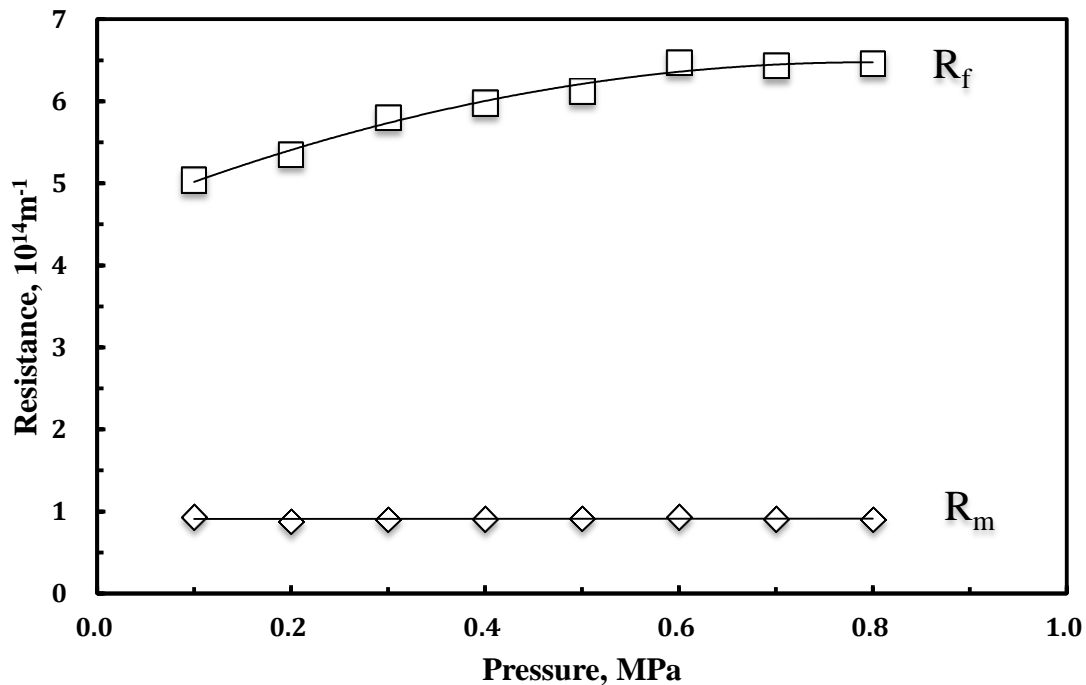


Figure 4.12 Membrane and fouling resistances as a function of pressure, Membrane NF-45

It is observed that for all five NF membranes, the membrane resistance  $R_m$  is always much smaller than the fouling resistance. The magnitude of membrane resistance depends on the membrane thickness and microporous structure (e.g., tortuosity, porosity, and pore size distribution). As expected, the fouling resistance increases with operating pressure and then gradually level off. This is understandable because as transmembrane pressure increases, more solutes are transported towards membrane surface, which causes solute accumulation on the membrane surface, leading to adsorption, pore blocking and concentration polarization until a steady state is reached. This tendency is consistent with the observed variations in the permeate flux and retention.

In order to compare the significance of membrane fouling for all the five NF membranes used in caprolactam separation, the ratio of  $R_f$  over  $R_{total}$  as a function of operating pressure was calculated as shown in Figure 4.13.

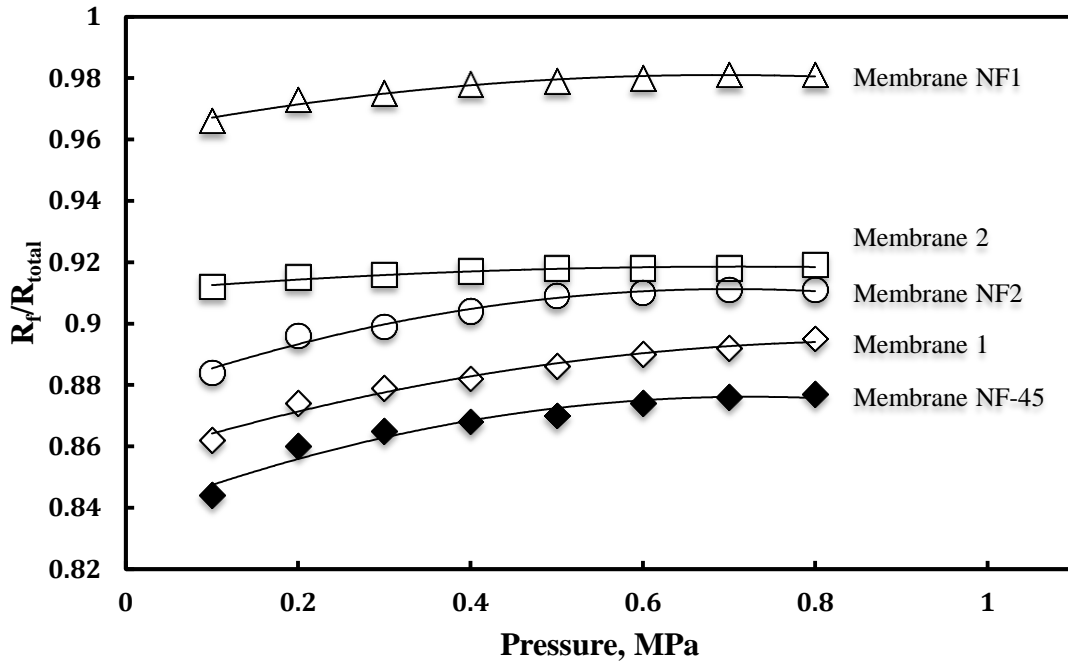


Figure 4.13  $R_f/R_{total}$  ratio for various NF membranes as a function of operating pressure

The data in Figure 4.13 shows that the significance of membrane fouling varied considerably from one membrane to another at given fouling operating conditions. The fouling severity was observed to be in the order of Membrane NF1 > Membrane 2 > Membrane NF2 > Membrane 1 > Membrane NF-45.

In addition, the fouling resistance for the 5 NF membranes as a function of feed caprolactam concentration was also analyzed at a given pressure (0.8MPa), and the results are shown in Figure 4.14.

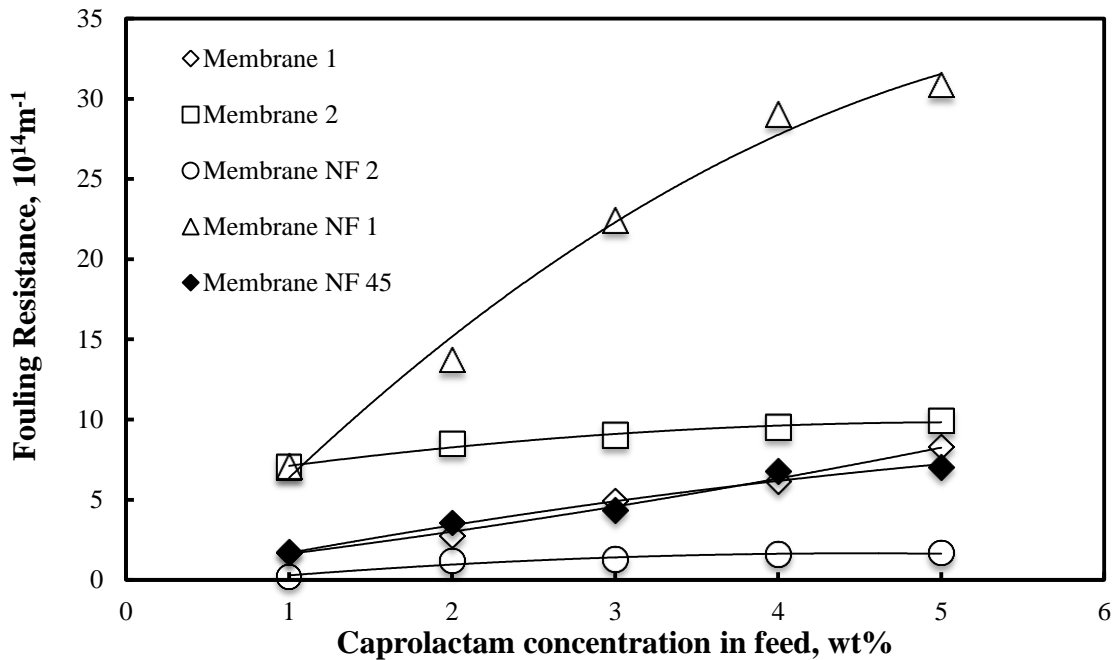


Figure 4.14 Variation of fouling resistances as function of feed caprolactam concentration at a pressure of 0.8MPa

As expected, the fouling resistance of the membrane increases with an increase in the feed caprolactam concentration, and over the 1-5% caprolactam feed concentration range tested, the fouling resistance of the NF membranes follows the order of Membrane NF1>Membrane 2>Membrane NF-45≈Membrane 1>Membrane NF2.

As mentioned previously, membrane fouling can be either reversible or irreversible, depending on the fouling mechanisms and cleaning techniques. Membrane fouling is considered to be reversible if the permeation flux can be recovered by backwashing, and otherwise it is irreversible fouling if the flux is not recovered after backwashing of the membrane. In the later case, the membrane normally needs to be cleaned by chemical reagents to recover its performance. Generally, only a portion of the overall membrane

fouling is reversible.

In order to investigate the reversibility of membrane fouling for caprolactam separation by the NF membrane process, a series of batch tests was conducted with Membrane NF1, which had the largest fouling resistance among all the NF membranes tested in this work. During these experiments, both permeate flux and permeate concentration of caprolactam were measured as a function of operating time at 0.8MPa and 1% feed caprolactam concentration. Each fouling test was run continuously for 7 hours, then the concentrated feed solution was taken out of the permeation cell and the membrane was washed by distilled water, followed by another batch run with fresh feed (1wt% caprolactam). 200ml of feed solution was charged to the permeation cell for each batch experiment. The test results are shown in Figure 4.15.

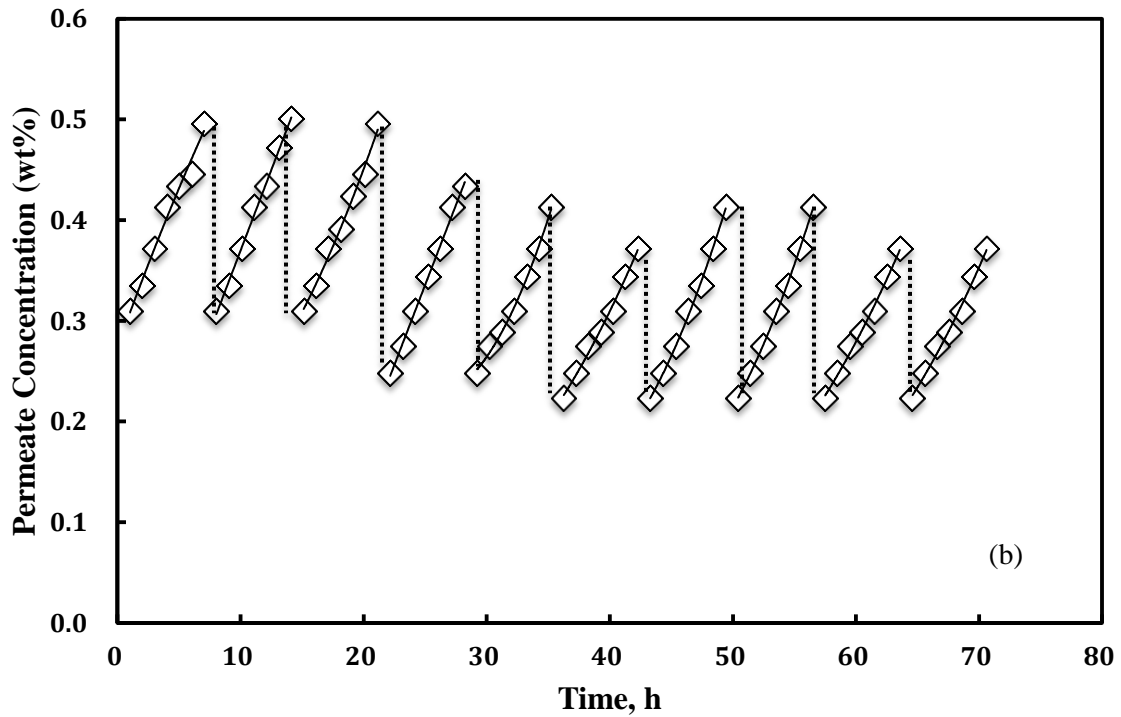
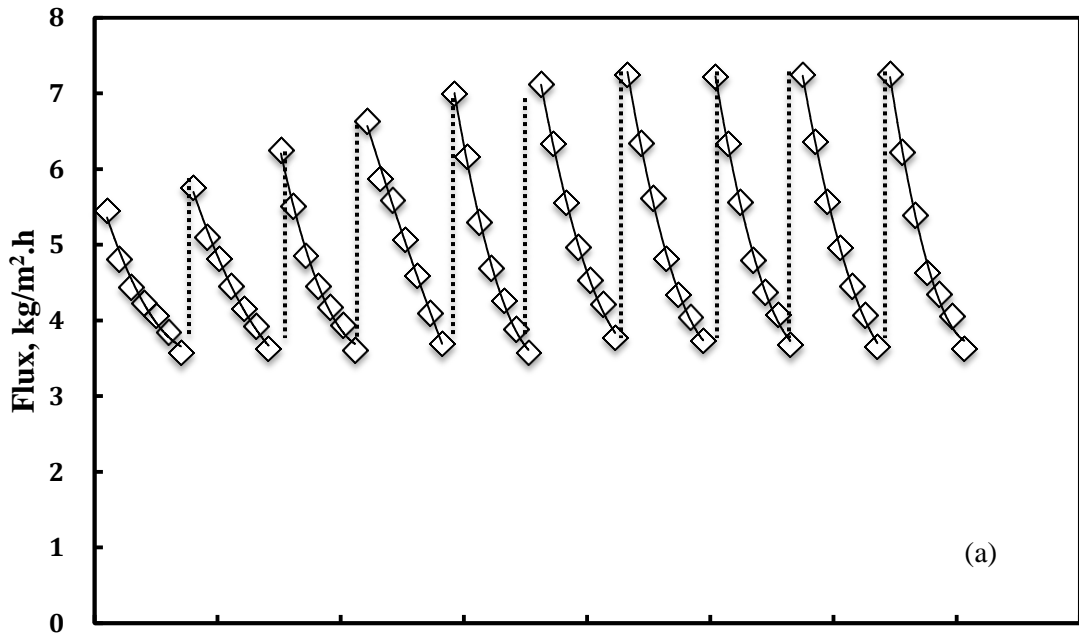


Figure 4.15 Permeation flux (a) and permeation concentration (b) as a function of operating time, Membrane NF1, 1wt% feed caprolactam. Membrane was washed with distilled water between batch NF runs

It's clear that both flux and concentration of caprolactam in the permeate varied with operating time. The permeate flux could decrease by nearly 35% after 7 hours of permeation, and the permeate caprolactam concentration could increase by 60%. When the membrane was washed by distilled water after each set of continuous NF experiments, the permeation flux and permeate caprolactam concentration can be restored to a large extent as compared to the initial values. All these suggest that the fouling during caprolactam separation using Membrane NF1 is essentially reversible, and the membrane performance can be recovered by washing with water.

Interestingly, when washed by distilled water after each set of NF batch tests, the permeate flux and caprolactam rejection were slightly higher than the initial values and they gradually became constant thereafter. This tendency once again proves the interaction between of caprolactam and the NF membrane materials due to their affinity. If this effect is too strong, deformation of active pore layer of the membrane materials may happen when caprolactam is adsorbed onto the surface and inner pores of the membrane.

## **4.2 Pervaporation**

The purpose of pervaporation was initially to isolate caprolactam from water based on its affinity to nylon 6 because caprolactam is the precursor of nylon 6. Unfortunately, it was found that caprolactam did not permeate through nylon membrane preferentially



presumably due to the low saturated vapor pressure and bulky structure of caprolactam molecules. In fact, the test result showed that under an operating temperature 25°C at a feed caprolactam concentration of 3wt%, the pervaporative separation factor of caprolactam over water was 0.261, which indicated that water actually permeated through the membrane preferentially, that is, the water to caprolactam separation factor is  $1/0.261=3.8$ . The contact angles of water on nylon 6 membrane was measured to be 61.2°, which indicated the degree of hydrophilicity of nylon 6. Additionally, the permeation flux for pervaporative removal of water is 0.497 kg/(m<sup>2</sup>.h), which is typical magnitude of non-porous pervaporation membranes.

Consequently, it is not feasible to use nylon membrane for permeating caprolactam from water by pervaporation for removal of caprolactam from wastewater. As a result, the research is shifted to membrane distillation, which uses microporous membrane for water removal at a much higher permeation rate.

### **4.3 Vacuum membrane distillation**

VMD was found to be promising as a high degree of separation was obtained (caprolactam rejection > 99.9%). In other words, caprolactam molecules are almost completely rejected by the microporous PTFE membrane thanks to the smaller sizes and more importantly, the higher volatility of water molecules. A comparison of water and caprolactam properties is presented in Table 4.1.

Table 4.1 Comparison of caprolactam and water properties

<b>Property</b>	<b>Caprolactam</b>	<b>Water</b>
Molecular weight (g/mol)	113.16	18.01
Boiling point (°C) @ 1atm	270.8	100
Saturated vapour pressure (Pa) @ 25 °C	0.28	3169
Density (g/cm <sup>3</sup> ) @ 25 °C	1.01	1

The effects of feed caprolactam concentration and operating temperature on the performance of VMD for water removal from the aqueous caprolactam solution were studied. Moreover, the potential fouling and concentration polarization during VMD were also investigated.

#### **4.3.1 Effect of operating conditions on VMD performance**

The hydrophobicity of the membrane is very important during VMD for water removal because ideally only vapor molecules are allowed pass membrane, while avoiding liquid penetration in membrane pores in order to minimize the mass transfer resistance. The contact angle of water on the PTFE membrane was measured to be is 164°, indicating that the PTFE membrane used is indeed highly hydrophobic and is ideal for use in the VMD process for removing water from the aqueous caprolactam solution, thereby concentrating the caprolactam.

Since it is much difficult to vaporize than water molecule, caprolactam is readily

rejected by the PTFE membrane during VMD. Flux and rejection were used to characterize the performance of the VMD process. In addition, water vapor permeance ( $\text{mol/m}^2 \cdot \text{s} \cdot \text{Pa}$ ) was used to characterize the permeability of the membrane to water vapor. The permeance is equal to permeation flux normalized by the driving force (pressure difference) across membrane.

When caprolactam concentration in the feed increases, the activity coefficient of water decreases, which will decrease the saturated vapor pressure of water and lead to a decline in water permeation rate. However, for the relatively low caprolactam concentrations (i.e., 0-5 wt%), the variations in activity coefficient of water are insignificant. As a result, there would not be much difference in water permeation flux over a small range of caprolactam concentration (0-5 wt%) (Mokbel, 1997).

Temperature is an important factor in VMD because it determines the saturated vapor pressure of the feed. Generally, permeate flux increases with increasing temperature since the penetrant molecules get more energetic at higher temperatures. Figures 4.16 and 4.17 show permeation flux of water and membrane permeance to water vapor permeation, respectively, as a function of reciprocal temperature over a temperature range from 25 to 65°C at different caprolactam concentrations in the feed (1-20 wt%).

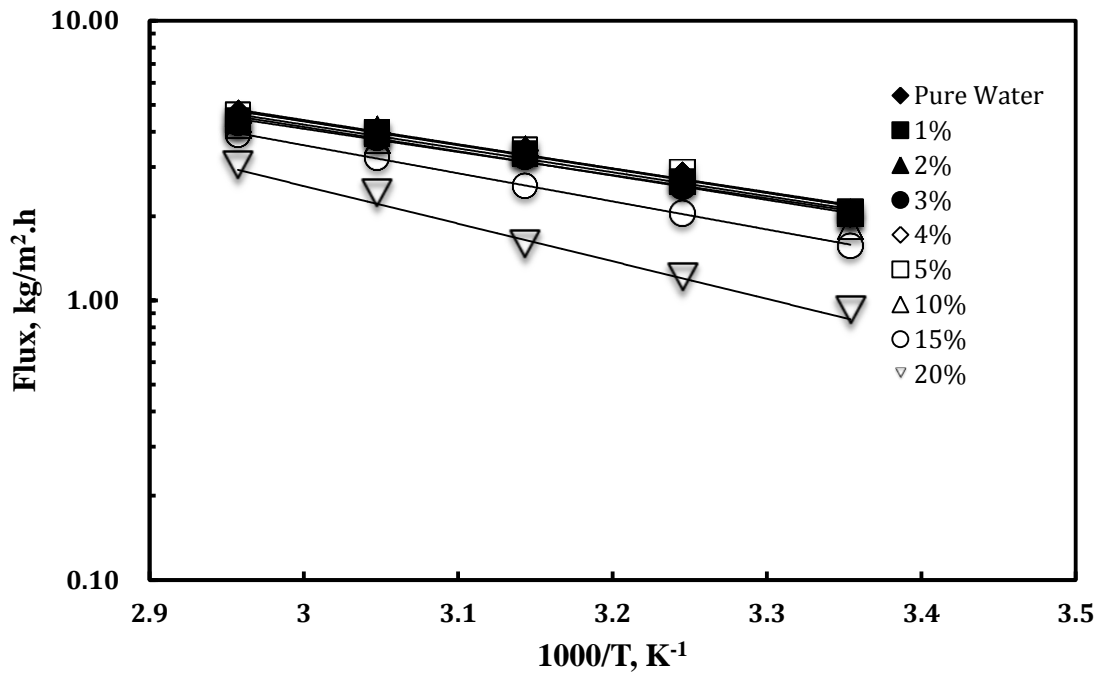


Figure 4.16 Effects of temperature on water permeation flux in the PTFE membrane

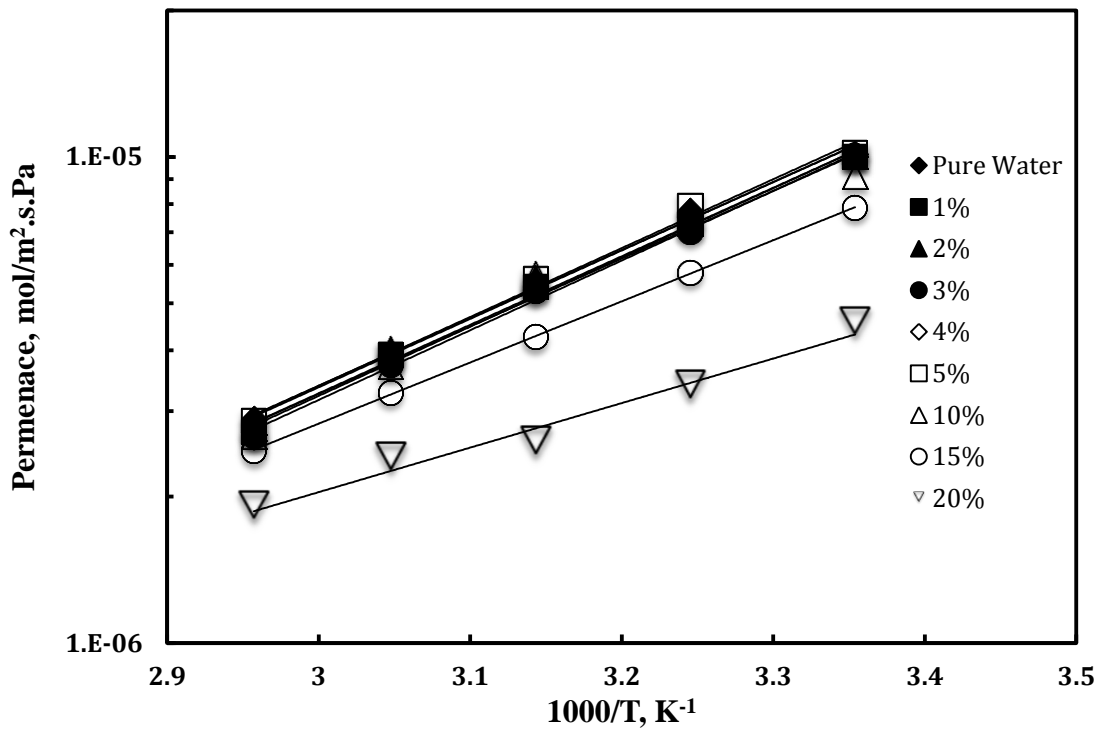


Figure 4.17 Effects of temperature on water permeance in the PTFE membrane

At 3 wt% feed caprolactam solution, the permeation flux of water under 25°C is 2.05 kg/(m<sup>2</sup>.h), which is much higher than that obtained with PV using nylon 6 membrane under same operating conditions (0.497 kg/m<sup>2</sup>.h). VMD uses porous and hydrophobic membranes, which act only as support for the vapor–liquid interface, while pervaporation requires dense membranes and the separation occurs based on relative solubility and diffusivity of each component in the membrane material.

The temperature dependence of the water permeation rate follows an Arrhenius type of relationship (Feng and Huang, 1996). There is a linear relationship between logarithmic permeation flux with reciprocal temperature, and the activation energy for permeation can be calculated from the slope of the straight line. The activation energy was shown to vary from 16 kJ/mol for 1 wt% feed caprolactam concentration to 25.7 kJ/mol for 20 wt% feed concentration.

As expected, the permeation flux increases with temperature at given feed caprolactam concentrations. Based on Antoine equation, the vapour pressure of water increases exponentially with temperature, and so is the driving force for mass transfer across the membrane (Alklaibi and Lior, 2005). In addition, for VMD, the vapor permeation through the membrane is governed by Knudsen diffusion. An increase in temperature will also increase the diffusion coefficient, which favors water vapor permeation (Srisurichan et al., 2006).

On the other hand, the permeability or permeance of the membrane declines with feed temperature. It can thus be concluded that the increase in permeation flux with

increasing temperature is ascribed to the increased driving force for permeation that over compensated for the decrease in membrane permeability. These results are in agreement with other work reported in the literature (Xu et al., 2010).

Over a low feed caprolactam concentration range (1-5 wt%), the membrane performance is not affected by the feed caprolactam concentration because the saturated water vapor pressure is essentially a constant over this concentration range. However, at a higher feed caprolactam concentration, the permeation flux and permeance of water will decrease considerably due to the decrease in activity coefficient of water, which lowers the saturated water vapor pressure over the feed solution. In addition, a reduction in permeation performance with increasing feed concentration can also be ascribed to decrease in the mass transfer coefficient in the liquid boundary layer at the feed side near the membrane surface because of concentration polarization (Lawson and Lloyd, 1997). The effects of feed caprolactam concentration on water permeation performance are more clearly shown in Figures 4.18 and 4.19.

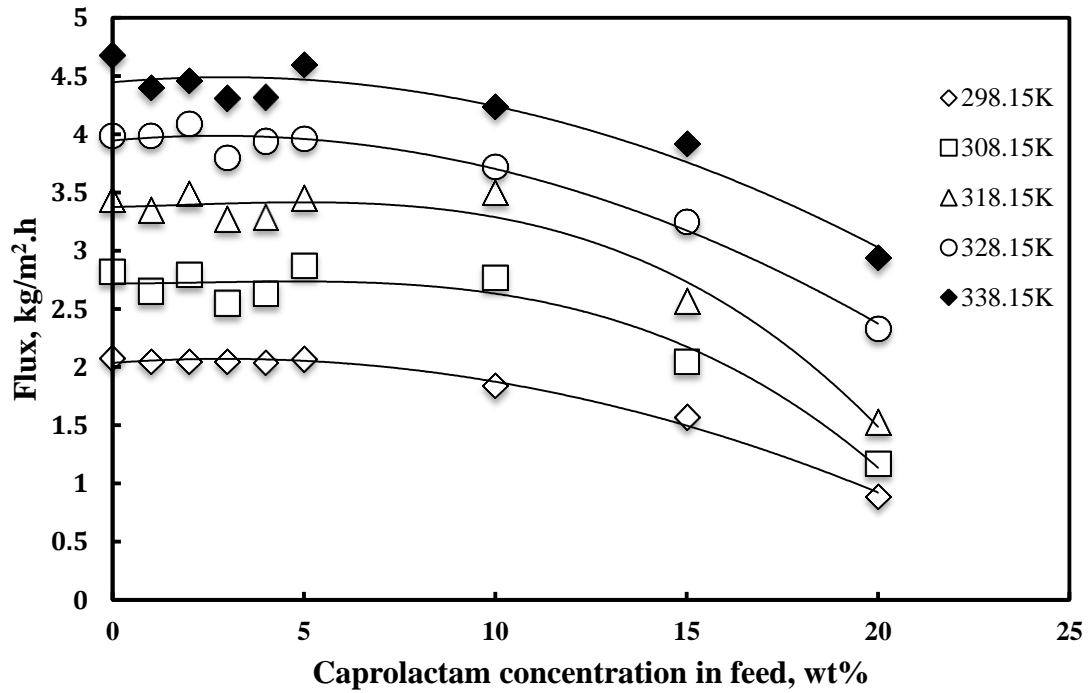


Figure 4.18 Effects of feed concentration on water permeation flux in the PTFE membrane

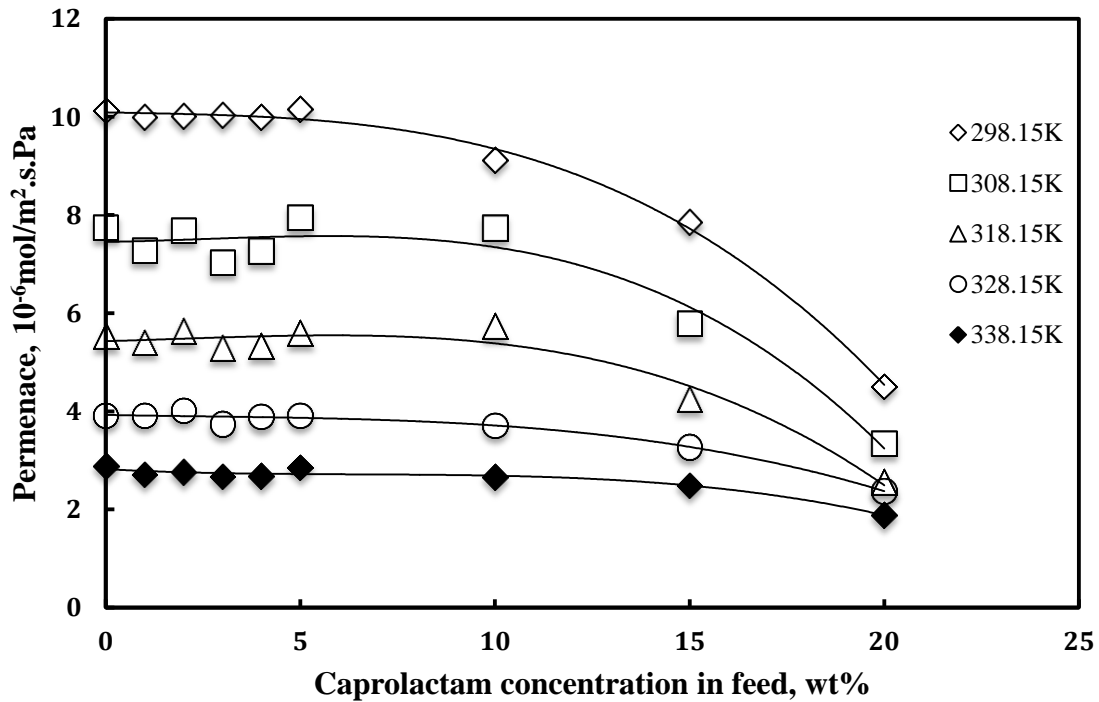


Figure 4.19 Effects of feed concentration on water permeance in the PTFE membrane

### **4.3.2 Concentration of aqueous solutions of caprolactam by VMD**

As mentioned before, solvent extraction and vacuum evaporation were mainly used to treat caprolactam-containing wastewater. However, because of low concentration of caprolactam in the wastewater, a large amount of energy will be consumed. VMD is shown to be promising for caprolactam concentration, and the concentrated caprolactam solution can be further purified by the conventional separation methods. The whole process to treat caprolactam wastewater will be more energy efficient. Therefore, batch operation of concentration experiment with 200 ml of 1 wt% caprolactam feed aqueous solutions at 65°C was conducted to investigate performance of VMD with time.

Figures 4.20 and 4.21 show the permeate flux and caprolactam concentration in the feed as function of operating time when water is continuously removed by VMD. The concentration experiment of caprolactam aqueous solution was conducted for 35.5 hours until the initial 200ml caprolactam solution (1 wt%) was completely distilled. Over a considerably long operating time, the water permeation flux is around 4.3 kg/m<sup>2</sup>.h within the first 32 hours, which is in agreement with the permeation data at different caprolactam concentrations. Over the entire period, the permeate is essentially pure water and did not deteriorate. During the first 32 hours, the caprolactam solution was concentrated from 1 wt% to nearly 6 wt%, while there were not much changes in permeation flux. This tendency consistent with the data in Figure 4.18. These results suggest that there was not much fouling and concentration polarization during VMD



except when the caprolactam concentration is highly concentrated. At the end of VMD for 35 hours, the feed caprolactam concentration reached 10.7 wt%, and the retention of PTFE membrane remained stable for whole period of operation (100%). Near the end of VMD, the flux decline may be attribute to the formation of a deposit layer of caprolactam on membrane surface and causes clogging of the pore channels, which will lead to an increase in permeation resistance. Additionally, partial membrane wetting may also occur as liquid may penetrate the deposited surface of adjacent pores.

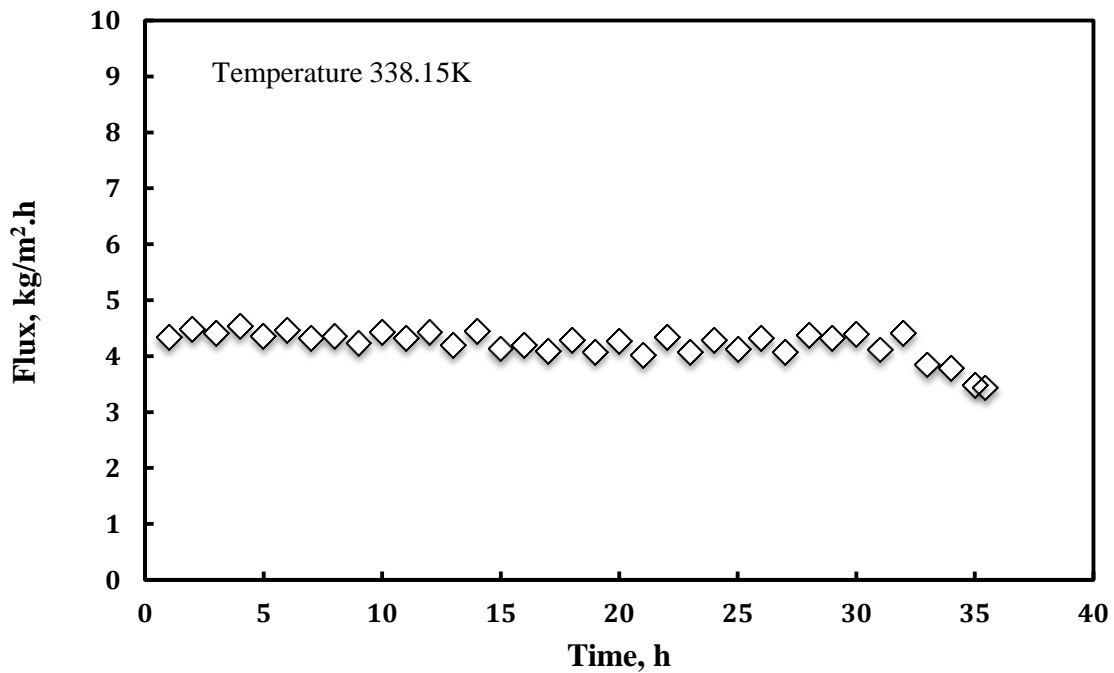


Figure 4.20 The permeation flux as a function of operating time, initial feed caprolactam concentration, 1 wt%

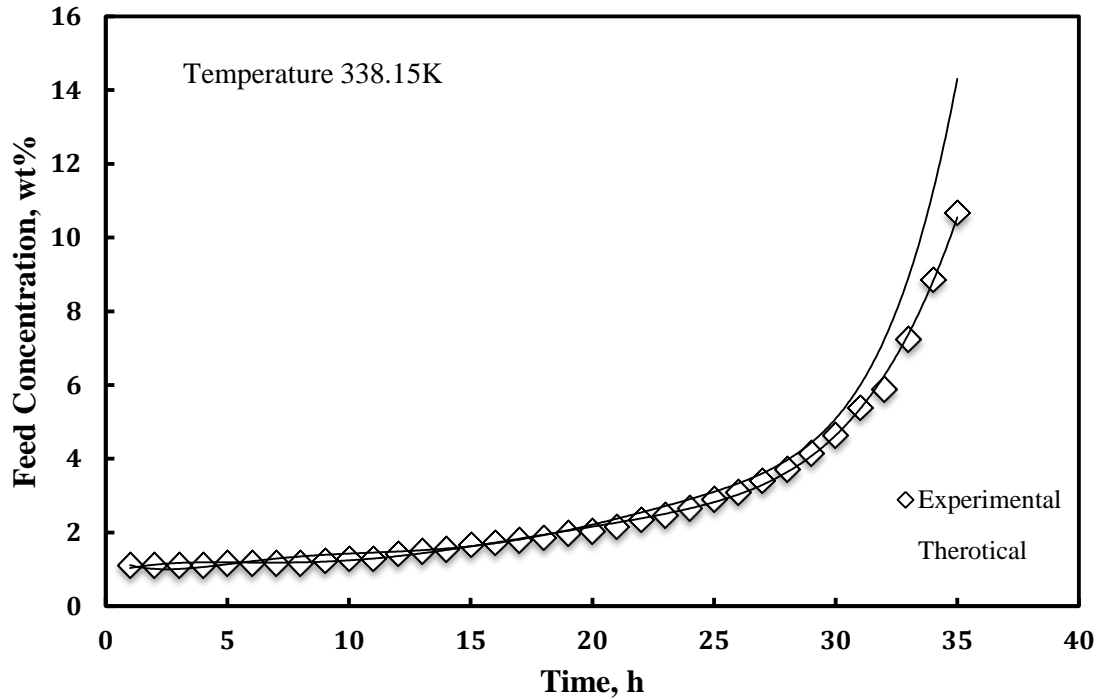


Figure 4.21 Concentration of caprolactam aqueous solution as a function of operating time, initial feed caprolactam concentration 1wt%

The experimental data of feed caprolactam concentration in Figure 4.21 also support the above explanations. A high concentration of that caprolactam will flocculate and deposit on the membrane surface during concentration of the solution. During continuous VMD operation, the permeation flux as well as feed caprolactam concentration was measured every hour. The feed concentration can be calculated by mass balance as shown in Figure 4.21 to confirm that the mass is balanced in spite of the numerous samples involved in the measurements.

Similar result has also been reported by Gryta, who used multistage membrane distillation to concentrate caprolactam solutions using a capillary membrane (Gryta, 2006). During the caprolactam concentration process, the formation of caprolactam

deposits on the membrane surface and accumulation of crystalline deposits in the feed tank were also detected. Figure 4.22 shows the SEM image of the deposit formed on the membrane surface.

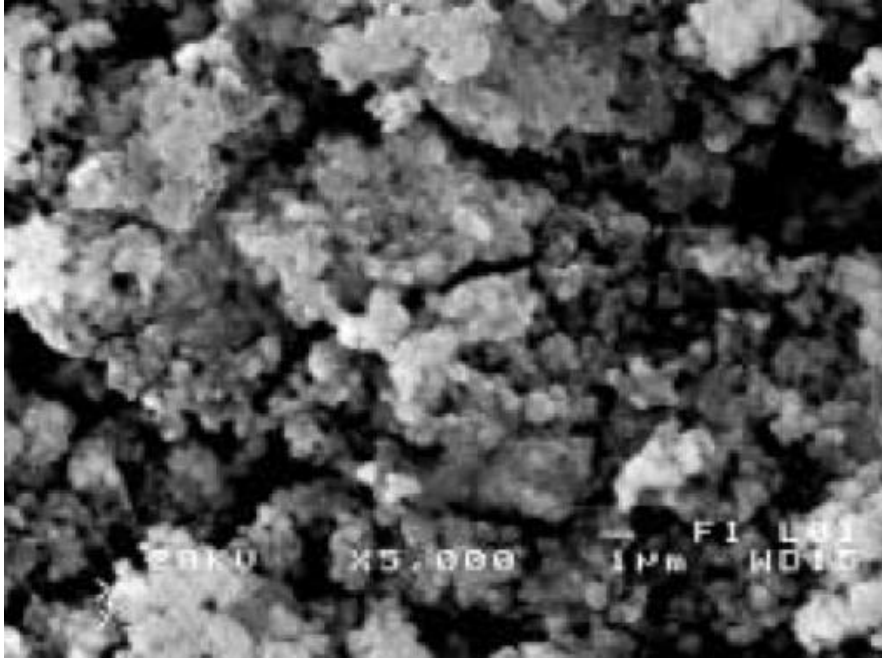


Figure 4.22 SEM image of the deposit formed on the membrane surface during the concentration of caprolactam solutions (Gryta, 2006)

## **Chapter 5 General conclusions and recommendations**

### **5.1 General conclusions**

The following conclusions can be drawn from this study.

(1) Nanofiltration (NF) was conducted using 5 different NF membranes, and the highest rejection was over 70% for separation of caprolactam solutions. The effects of operating conditions (i.e., operating pressure 0.1-0.8 MPa and feed concentration 1-5 wt%) on the NF performance were studied. An increase in pressure could improve permeate productivity, but membrane fouling was shown to be significant. The fouling resistances of the membranes are in the following order: Membrane NF1>Membrane 2>Membrane NF-45>Membrane 1>Membrane NF2. The membrane fouling during NF of caprolactam solutions was found to be reversible and the membrane performance could be recovered by washing with distilled water. In addition, Membrane NF-45 was shown to behave differently from the other 4 NF membranes.

(2) The performance of pervaporation (PV) to separate caprolactam from water by nylon 6 membrane was poor. In spite of the good affinity between caprolactam and nylon 6, water was found to preferentially permeate through the membrane, and the selectivity was very limited.

(3) Vacuum membrane distillation (VMD) was found to be effective to concentrate caprolactam solution. Due to its much lower volatility than water, only water was

permeable through the membrane, and a complete retention of caprolactam was observed. Increasing temperature could enhance the water productivity remarkably. At a given temperature, the water flux was essentially independent of the feed concentration for feed caprolactam concentration below 5 wt%. Fouling occurs when the caprolactam aqueous solution became substantially concentrated, and any deposit on the membrane surface would decrease the water flux considerably.

## **5.2 Recommendations**

Based on the research findings from this work, the followings are recommended for further study:

(1) Although a rejection rate of up to 70% can be achieved with NF, which is high for typical separation of organics-water mixtures by NF. A further separation is needed for the wastewater treatment. This can be done by using multistage NF or a hybrid process combining NF with liquid-liquid extraction. The permeate from NF still contains a smaller amount of caprolactam, which can be treated with reverse osmosis membranes. In addition, chemical modifications of the NF membranes are needed to reduce membrane fouling. Furthermore, because of the affinity between caprolactam and amide groups in interfacially formed polyamide NF membranes, studies of the interactions between them and how the interactions influence membrane surface property and structure will be of interest to have a better understanding of the NF process.

(2) High retention of caprolactam by VMD is confirmed in the study. It is

recommended to look into a hybrid process that use liquid-liquid extraction to recover caprolactam from the concentrated caprolactam solution generated by the VMD. Moreover, although the influence of operating conditions on the performance of VMD has been studied, a further research on the durability, processing capacity and scale up of the process will be useful to provide additional information on process design.

## References

Alkudhiri, A., N. Darwish and N. Hilal, Membrane distillation: A comprehensive review, *Desalination*,287(2012)2-18.

Alklaibi, A.M. and N. Lior, Membrane-distillation desalination: Status and potential, *Desalination*,171(2005)111-131.

Arora, A., B.S. Dien, R.L. Belyea, P. Wang, V. Singh, M.E. Tumbleson and K.D. Rausch, Thin stillage fractionation using ultrafiltration: resistance in series model, *Bioprocess. Biosyst. Eng.*,32(2009)225-233.

Baker, R.W., *Membrane Separation Systems - Recent Developments and Future Directions*, William Andrew Publishing/Noyes, 1991

Baker, R.W., *Membrane technology and application*, John Wiley & Sons, Ltd, West Sussex, England,2004

Banat, F.A. and J. Simandl, Theoretical and experimental study in membrane distillation, *Desalination*,95(1994)39-52.

Bandini, S. and G.C. Sarti, Heat and mass transport resistances in vacuum membrane distillation per drop, *AIChE*,45(1999)1422-1433.

Baxi, N.N. and A.K. Shah,  $\epsilon$ -Caprolactam-degradation by *Alcaligenes faecalis* for bioremediation of wastewater of a nylon-6 production plant, *Biotechnol. Lett.*,24(2002)1177-1180.

Beasley, J.K. and R.E. Penn, Hollow fine fiber vs. flat sheet membranes-A comparison of structures and performance, *Desalination*,38(1981)361-372.

Bernardo, P., E. Drioli and G. Golemme, Membrane gas separation a review:state of the art, *Ind. Eng. Chem. Res.*,48(2009)4638 – 4663.

Blume, I., J.G. Wijmans and R.W. Baker, The separation of dissolved organics from water by pervaporation, *J. Membr. Sci.*,49(1990)253-286.

Bowen, T.C., R.D. Noble and J.L. Falconer, Fundamentals and applications of pervaporation through zeolite membranes, *J. Membr. Sci.*,245(2004)1-33.

Bowen, W.R. and H. Mukhtar, Characterisation and prediction of separation performance of nanofiltration membranes, *J. Membr. Sci.*,112(1996)263-274.

Brandrup, J., *Polymer Handbook*, John Wiley & Sons, 1999

Chen, D., X. OuYang, Y. Wang, L. Yang and C. He, Liquid–liquid extraction of caprolactam from water using room temperature ionic liquids, *Sep. Purif. Technol.*,104(2013)263-267.

Denisova, G.P., S.E. Artemenko, T.P. Ustinova, L.L. Zhuravleva and O.M. Sladkov, Ultrafiltration membranes for removal of caprolactam from industrial discharges, *Fibre Chem.*,31(1999)168-170.

Dupont, Fluoroplastic Comparison - Typical Properties. from [http://www2.dupont.com/Teflon\\_Industrial/en\\_US/tech\\_info/techinfo\\_compare.html](http://www2.dupont.com/Teflon_Industrial/en_US/tech_info/techinfo_compare.html).

2006

Fang, W., L. Shi and R. Wang, Interfacially polymerized composite nanofiltration hollow fiber membranes for low-pressure water softening, *J. Membr. Sci.*,430(2013)129-139.

Feng, X. and R.Y.M. Huang, Estimation of activation energy for permeation in pervaporation processes, *J. Membr. Sci.*,118(1996)127-131.



Feng, X. and R.Y.M. Huang, Liquid separation by membrane pervaporation a review, *Ind. Eng. Chem. Res.*,36(1997)1048-1066.

Franken, A.C.M., J.A.M. Nolten, M.H.V. Mulder, D. Bargeman and C.A. Smolders, Wetting criteria for the applicability of membrane distillation, *J. Membr. Sci.*,33(1987)315-328.

Frarès, N.B., S. Taha and G. Dorange, Influence of the operating conditions on the elimination of zinc ions by nanofiltration, *Desalination*,185(2005)245-253.

George, S.C. and S. Thomas, Transport phenomena through polymeric systems, *Prog. Polym. Sci.*,26(2001)985-1017.

Gryta, M., Concentration of aqueous solutions of caprolactam by membrane distillation, *Polimery*,51(2006)665-670.

Hilal, N., H. Al-Zoubi, N.A. Darwish, A.W. Mohamma and M. Abu Arabi, A comprehensive review of nanofiltration membranes:Treatment, pretreatment, modelling, and atomic force microscopy, *Desalination*,170(2004)281-308.

Hilal, N., O.O. Ogunbiyi, N.J. Miles and R. Nigmatullin, Methods Employed for Control of Fouling in MF and UF Membranes: A Comprehensive Review, *Separation Science and Technology*,40(2005)1957-2005.

Holmes, S.M., M. Schmitt, C. Markert, R.J. Plaisted, J.O. Forrest, P.N. Sharratt, A.A. Garforth, C.S. Cundy and J. Dwyer, Zeolite a Membranes for Use in Alcohol/Water Separations, *Chem. Eng. Res. Des.*,78(2000)1084-1088.

Hong, J. and X. Xu, Environmental impact assessment of caprolactam production – a case study in China, *J. Cleaner Production*,27(2012)103-108.

Hwang, S.T., Fundamentals of membrane transport, *Korean J. Chem. Eng.*,28(2010)1-15.

Ismail, A.F. and A.R. Hassan, The deduction of fine structural details of asymmetric nanofiltration membranes using theoretical models, *J. Membr. Sci.*,231(2004)25-36.

Ismail, A.F. and A.R. Hassan, Formation and characterization of asymmetric nanofiltration membrane: Effect of shear rate and polymer concentration, *J. Membr. Sci.*,270(2006)57-72.

Iwata, H., M. Oodate and Y. Uyama, Preparation of temperature sensitive membranes by graft-polymerization onto a porous membrane, *J. Membr. Sci.*,55(1991)119-130.

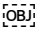
Kaya, Y., H. Barlas and S. Arayici, Evaluation of fouling mechanisms in the nanofiltration of solutions with high anionic and nonionic surfactant contents using a resistance-in-series model, *J. Membr. Sci.*,367(2011)45-54.

Khayet, M. and T. Matsuura, Pervaporation and vacuum membrane distillation processes: Modeling and experiments, *AIChE*,50(2004)1697-1712.

Kulkarni, R.S. and P.P. Kanekar, Bioremediation of e-caprolactam from Nylon-6 wastewater by use of *Pseudomonas aeruginosa* MCM B-407, *Curr. Microbiol.*,37(1998)191-194.

Lau, W. and A.F. Ismail, Polymeric nanofiltration membranes for textile dye wastewater treatment: Preparation, performance evaluation, transport modelling, and fouling control — a review, *Desalination*,245(2009)321-348.

Lawson, K.W. and D.R. Lloyd, Membrane distillation, *J. Membr. Sci.*,124(1997)1-25.

Lonsdale, H.K., The growth of membrane technology, *J. Membr. Sci.*,10(1982)81-181.

Mallick, S. and B.B. Khatua, Morphology and properties of nylon6 and high density polyethylene blends in absence and presence of nanoclay, *J. Appl. Polym. Sci.*,121(2011)359-368.

Marín, N.G. and J.A. López-Ramírez, Influence of organic fouling and operating conditions on nanofiltration membranes to reduce phenol concentration in natural waters, *Water Sci. Technol.*,11(2011)473.

Mehiguene, K., Y. Garba, S. Taha, N. Gondrexon and G. Dorange, Influence of operating conditions on the retention of copper and cadmium in aqueous solutions by nanofiltration experimental results and modelling, *Sep. Purif. Technol.*,15(1999)181-187.

Mokbel, I., S. Ye, J. Jose and P. Xans, Study of non ideality of various aqueous sodium chloride solutions by vapor pressures measurements and correlation of experimental results by Pitzer's method, *J. Chem. Phys.*,94(1997)122-137.

Mulder, M., *Basic Principles of Membrane Technology*, Kluwer Academic Publishers, Netherlands,1991

Noble, R.D., *An Overview of Membrane Separations*, *Sep. Sci. Technol.*,22(1987)731-743.

Nunes, S.P., M.L. Sforca and K.V. Peinemann, Dense hydrophilic composite membranes for ultrafiltration, *J. Membr. Sci.*,106(1995)49-56.

Oatley, D.L., L. Llenas, R. Perez, P.M. Williams, X. Martinez-Llado and M. Rovira, Review of the dielectric properties of nanofiltration membranes and verification of the single oriented layer approximation, *Adv. Colloid Interf. Sci.*,173(2012)1-11.

Okushita, H., M. Yoshikawa and T. Shimidzu, Synthesis of polyoxyethylene grafting nylon 6, *J. Membr. Sci.*,112(1996)91-100.

Pangarkar, B.L., P.V. Thorat, S.B. Parjane and R.M. Abhang, Performance evaluation of vacuum membrane distillation for desalination by using a flat sheet membrane, *Desalin. Water Treat.*,21(2010)328-334.

Peuchot, M.M. and R.B. Aim, Improvement of cross-flow microfiltration performances with flocculation, *J. Membr. Sci.*,68(1992)241-248.

Pinnau, I. and B.D. Freeman, Formation and Modification of Polymeric Membranes: Overview, ACS Symposium Series, Washington, DC., America,1999

Sarti, G.C., C. Gostoli and S. Bandini, Extraction of organic components from aqueous streams by vacuum membrane distillation, *J. Membr. Sci.*,80(1993)21-33.

Schäfer, A.I., A.G. Fane and W.D. Thomas, Nanofiltration: Principles and Applications, Elsevier Science, 2005

Schneider, K., W. Hütz and R. Wollbeck, Membranes and modules for transmembrane distillation, *J. Membr. Sci.*,39(1988)25-42.

Shao, P. and R.Y.M. Huang, Polymeric membrane pervaporation, *J. Membr. Sci.*,287(2007)162-179.

Sheldon, T., Chromosomal damage induced by caprolactam in human lymphocytes, *Mutat. Res.*, 224(1989)325-327.

Shirazi, S., C. Lin and D. Chen, Inorganic fouling of pressure-driven membrane processes — A critical review, *Desalination*,250(2010)236-248.

Song, Y., F. Liu and B. Sun, Preparation, characterization, and application of thin film composite nanofiltration membranes, *J. Polym. Sci.*,95(2005)1251-1261.

Srisurichan, S., R. Jiraratananon and A. Fane, Mass transfer mechanisms and transport resistances in direct contact membrane distillation process, *J. Membr. Sci.*,277(2006)186-194.

Sun, J. and Y. Zhang, Modification of polytetrafluoroethylene by radiation—1.

Improvement in high temperature properties and radiation stability, *Radiat. Phys. Chem.*,44(1993)655–659.

Tu, S., V. Ravindran and M. Pirbazari, A pore diffusion transport model for forecasting the performance of membrane processes, *J. Membr. Sci.*,265(2005)29-50.

Van Delden, M.L., N.J.M. Kuipers and A.B.d. Haan, Selection and evaluation of alternative solvents for caprolactam extraction, *Sep. Purif. Technol.*,51(2006)219-231.

Van der Horst, H.C., J.M.K. Timmer, T. Robbertsen and J. Leenders, Use of nanofiltration for concentration and demineralization in the dairy industry Model for mass transport, *J. Membr. Sci.*,104(1995)205-218.

Van Krevelen, D.W., *Properties of Polymers*, Elsevier, Amsterdam, Netherlands,1972

Wang, X., T.Tsuru, S. Nakao and S. Kimura, Electrolyte transport through nanofiltration membranes by the space-charge model and the comparison with Teorell-Meyer-Sievers model, *J. Membr. Sci.*,103(1995)117-133.

Wijmans, J.G. and R.W. Baker, The solution-diffusion model a review, *J. Membr. Sci.*,107(1995)1-21.

Wilderer, P., *Treatise on Water Science*, Elsevier Science, 2011

William, M.H., D.R. Lide and T.J. Bruno, *CRC Handbook of Chemistry and Physics*, CRC Press, 2012

Winzeler, H.B. and G. Belfort, Enhanced performance for pressure-driven membrane processes the argument for fluid instabilities, *J. Membr. Sci.*,80(1993)35-47.

Xie, F.Y., M.Q. Zhu, J.Q. Liu and C.H. He, Extraction of caprolactam from aqueous ammonium sulfate solution in pulsed packed column using 250Y mellapak packings,

Chinese J. Chem. Eng.,10(2002)48-51.

Xu, J., C. Gao and X. Feng, Thin-film-composite membranes comprising of self-assembled polyelectrolytes for separation of water from ethylene glycol by pervaporation, J. Membr. Sci.,352(2010)197-204.

Yoshikawa, M. and K. Tsubouchi, Specialty polymeric membranes 10 Separation of benzene from benzene:cyclohexane mixtures with modified nylon 6 membranes, Sep. Purif. Technol.,17(1999)213-223.

Zhang, L., P. Yu and Y. Luo, Dehydration of caprolactam–water mixtures through cross-linked PVA composite pervaporation membranes, J. Membr. Sci.,306(2007)93-102.

## Appendix A Sample Calculations

### A.1 Resistance-in-series model calculations

The following calculations were conducted to evaluate the membrane resistance ( $R_m$ ) and fouling resistance ( $R_f$ ) of Membrane NF1 during nanofiltration running under 5 wt% feed caprolactam concentration and 0.8 MPa operating pressure at 25°C. The permeation flux of pure water and 5 wt% caprolactam in feed through Membrane NF 1 are 35.83 and 0.57 kg/(m<sup>2</sup>.h), respectively.

#### Resistance-in-series model

Use the resistance in series model introduced in Section 2.4.2:

$$R_m = \frac{\Delta P}{\mu_{water} \cdot J}$$

In order to estimate the fouling resistance, the total resistance was determined first:

$$R_{total} = \frac{\Delta P}{\mu_{solution} \cdot J}$$

$$R_f = R_{total} - R_m$$

where viscosities of pure water and 5% caprolactam solution at 25°C are 1.05 and 1.23 cp (10<sup>-3</sup> Pa.s), respectively.

$$R_m = \frac{0.8 \times 10^6 Pa}{1.05 \times 10^{-3} Pa \cdot s \times 35.83 \times 10^{-3} \div 3600 m^3 / (m^2 \cdot s)} = 7.66 \times 10^{13} m^{-1}$$

$$R_{total} = \frac{0.8 \times 10^6 Pa}{1.23 \times 10^{-3} Pa \cdot s \times 0.57 \times 10^{-3} \div 3600 m^3 / (m^2 \cdot s)} = 4.11 \times 10^{15} m^{-1}$$

$$R_f = 4.11 \times 10^{15} - 7.66 \times 10^{13} = 4.03 \times 10^{15} m^{-1}$$

## A.2 Permeance calculations

The following calculations were conducted to estimate the permeance of PTFE membrane during vacuum membrane distillation in separation of aqueous caprolactam solution under 1 wt% feed caprolactam concentration and 65°C operating temperature. The permeation flux of water through this membrane under such operating conditions was 4.4 kg/(m<sup>2</sup>.h). Then the permeance (Q) was evaluated using a pressure-normalized flux:

$$Q = \frac{J}{\Delta P}$$

the pressure on the feed side was generated by partial water vapor pressure:

$$P_1 = P_s \cdot X_{H_2O} \cdot \gamma$$

where P<sub>s</sub> is water vapor pressure at 65°C (25.02kPa), X<sub>H<sub>2</sub>O</sub> is the mole fraction of water in feed, γ is the water activity coefficient that is considered as 1 for dilute caprolactam solutions. As the pressure on the permeate side was maintained at 2 kPa, ΔP can be obtained as:



$$\Delta P = 25.02 \times \frac{\frac{99}{18}}{\left(\frac{99}{18} + \frac{1}{113.16}\right)} \times 1 \times 1000 - 2000 = 2.3 \times 10^4 \text{ Pa}$$

by convection, the flux unit  $\text{kg}/(\text{m}^2 \cdot \text{h})$ .

$$1 \frac{\text{kg}}{(\text{m}^2 \cdot \text{h})} = \frac{1 \times 1000}{18 \times 3600} \text{ mol}/\text{m}^2 \cdot \text{s}$$

$$Q = \frac{4.4}{18 \times 3.6 \times 2.3 \times 10^4} = 2.95 \times 10^{-6} \text{ mol}/(\text{m}^2 \cdot \text{s} \cdot \text{Pa})$$